ATBD-AST-08
ALGORITHM THEORETICAL BASIS DOCUMENT

FOR

ASTER DIGITAL ELEVATION MODELS
(STANDARD PRODUCT AST14)

VERSION 3.0

REVISED 5 FEBRUARY 1999

HAROLD R. LANG, JPL
ROY WELCH, UNIVERSITY OF GEORGIA

TABLE OF CONTENTS Page

LIST OF APPENDICES

LIST OF FIGURES

LIST OF TABLES

ACKNOWLEDGMENTS

This document is based on information and ideas developed by members of the ASTER Digital Elevation Model Working Group (ADEMWG) (Appendix 6-1). Work by the JPL ASTER Project Office, particularly that of Bob Hekl and Ron Cohen in the area of mission planning, has made this document possible. Geometric analysis of the ASTER stereo system by Kohei Arai, Saga University, Japan, provided essential information. USGS personnel at the Land DAAC, especially Bryan Bailey and Glenn Kelly, provided important operational input. Craig Leff and Nancy King, JPL, helped create the electronic version of this document that is on the EOS Project Science Office and ASTER home pages.

Earlier versions of this document were released 28 February 1994, 3 April 1995, and 16 August 1996 (Version 2.0, JPL D13751). These earlier versions were reviewed by EOS project panels chaired by Berrien Moore on 16 May 1994, and 10 December 1996. A SWAMP (Science Working Group AM Platform) panel chaired by John Miller reviewed the 3 April 1995 version on 16 May 1996. Constructive reviews of early drafts of this document by Hiroshi Murakami, Acting ADEMWG Co-Chair, and Mike Abrams, ASTER Team Associate, were helpful. Dean Gesch and Jim Conel provided written reviews as part of the EOS ATBD review process; their valuable suggestions have been incorporated. Written reviews by J. P. Muller and an anonymous reviewer also provided input. This, the fourth revision, incorporates corrections and additions based on all of these reviews as well as information from annual ADEMWG meetings.

The research described in this document was carried out in part at the Jet Propulsion Laboratory, California Institute of Technology, under contract with the National Aeronautics and Space Administration, and at the University of Georgia under contract with JPL. Reference herein to any specific commercial product, process or service by trade name, trademark, manufacturer, or otherwise does not constitute or imply endorsement by the United States Government or the Jet Propulsion Laboratory, California Institute of Technology.

1.0 Introduction

This document fulfills the EOS Project requirement as the Algorithm Theoretical Basis Document (ATBD) for the ASTER Digital Elevation Model (DEM) standard data product AST14. Not discussed here are plans for producing special data product DEMs at the Product Generation System facility in Japan, which are described in Welch et al. (1998) and documented in DWG (1997).

The outline and format of this ATBD were specified by the EOS Project Science Office. An electronic version of this document is available at: http://eospso.gsfc.nasa.gov. This document also serves as the ASTER Standard Product DEM Users Guide, a document that is being developed by the ADEMWG to serve as a basic reference for those interested in using ASTER stereo data and Standard Product DEMs. The Users Guide will be modified as is appropriate over the course of the EOS Project; a revised version will be reviewed by the ADEMWG during joint meetings of the ASTER Science Team. Information contained in this document was incorporated in a Request for

Proposals (RFP) released in February 1997 by the Land DAAC (USGS), for selecting a commercial system for deriving Standard Product DEMs from ASTER stereo data.

The Advanced Spaceborne Thermal Emission and Reflection Radiometer (ASTER) is a high-spatial-resolution multispectral imager currently scheduled for launch into Earth orbit in mid-1999, on the first platform of NASA's Earth Observing System (EOS AM1). Overviews of the entire ASTER system and ASTER experiment goals are provided by Kahle et al. (1991), Tsu et al. (1996), Yamaguchi et al. (1993), and Yamaguchi et al. (1998). Figure 1.0-1 illustrates how ASTER DEMs fit into the overall scheme of ASTER standard product generation.

A six year ASTER mission is planned. ASTER has an 8 minute/orbit duty cycle. The ASTER stereoscopic subsystem consists of nadir and rear-viewing telescopes operating in the visible-near infrared wavelengths. This subsystem, configured to provide a base-to-height ratio of 0.6, will acquire along-track, digital stereo data at 15 m resolution over a 60 km ground swath (Figure 1.0-2). Thus, ASTER incorporates capabilities for digital photogrammetry first proposed for the Stereosat (NASA, 1979) and Mapsat (Itek, 1981) mission concepts of the late 1970s.

This document describes the algorithm/process that will be used to produce standard product DEMs from along-track ASTER stereo data. These DEMs will be produced, after launch of the EOS AM platform, when ASTER Level 1 input data are available. Commercial off-the-shelf software, the PCI OrthoEngine, will be used to implement the automated, stereo correlation approach.

2.0 Objective and Background

Probably the most fundamental geophysical measurement of the planet Earth is the shape of the land surface. For hundreds of years, this has been the focus of the fields of cartography and geodesy. Literally all disciplines of scientific research involving the Earth's land surface require topographic data and derivative slope, slope aspect, and orthoimage cartographic products (Topographic Science Working Group, 1988; Gesch, 1993).

Production of geocoded, orthorectified raster images, a necessity for incorporating image data in a GIS database, requires DEM data (Hohle, 1996; Thorpe, 1996). Topographic information is also required for many of the geometric, radiometric and atmospheric corrections of satellite data from optical and microwave instruments. For example, correction of data from MODIS, MISR as well as ASTER itself requires use of the sort of digital topographic data that ASTER stereo can provide. These requirements are described in algorithm theoretical documents for the data products from those instruments. ASTER class DEMs are also required for two-look radar interferometry measurements of cm-scale Earth deformation due to earthquakes, volcanism or landslides (Gens and Van Genderen, 1996).

With its 8% duty cycle, ASTER is capable of acquiring a maximum of 771 stereo scenes/day. Because of mission operations and processing limitations, this maximum will not be realized. The first six months of the mission will be devoted primarily to system engineering, testing and ramping-up of Level 1 data production. Subsequently, the present plan calls for processing 310 ASTER scenes per day to

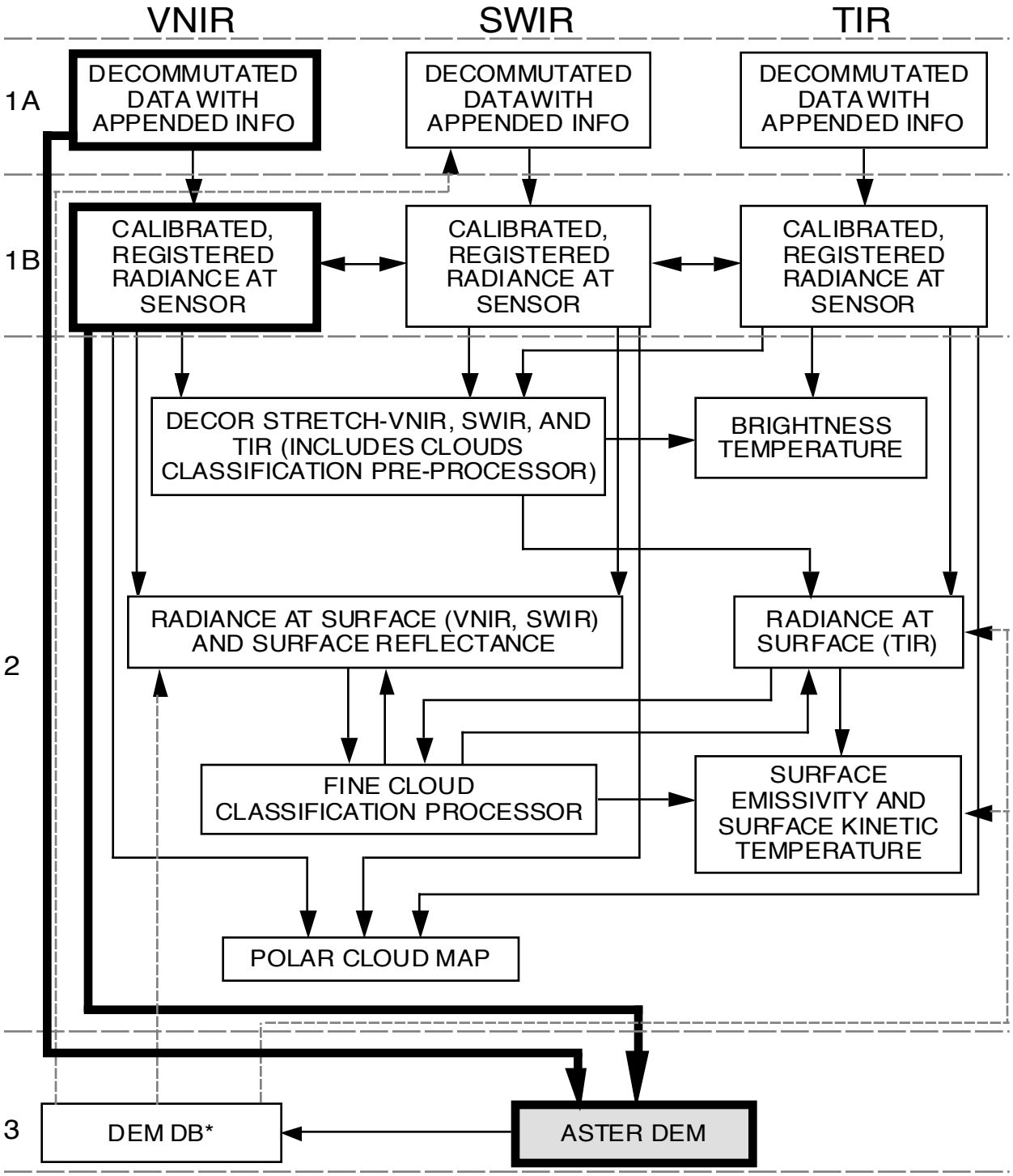

*REFERS TO A DATABASE OF DEM DATA REGARDLESS OF THE SOURCE

FIGURE 1.0-1. DIAGRAM SHOWING INTERDEPENDENCIES OF THE STANDARD ASTER DATA PRODUCTS. EITHER LEVEL 1A OR SOM-PROJECTED LEVEL 1B ASTER DIGITAL STEREOPAIRS FORMED BY VNIR BANDS 3N AND 3B ARE USED AS INPUT FOR ASTER DEM PRODUCTION.

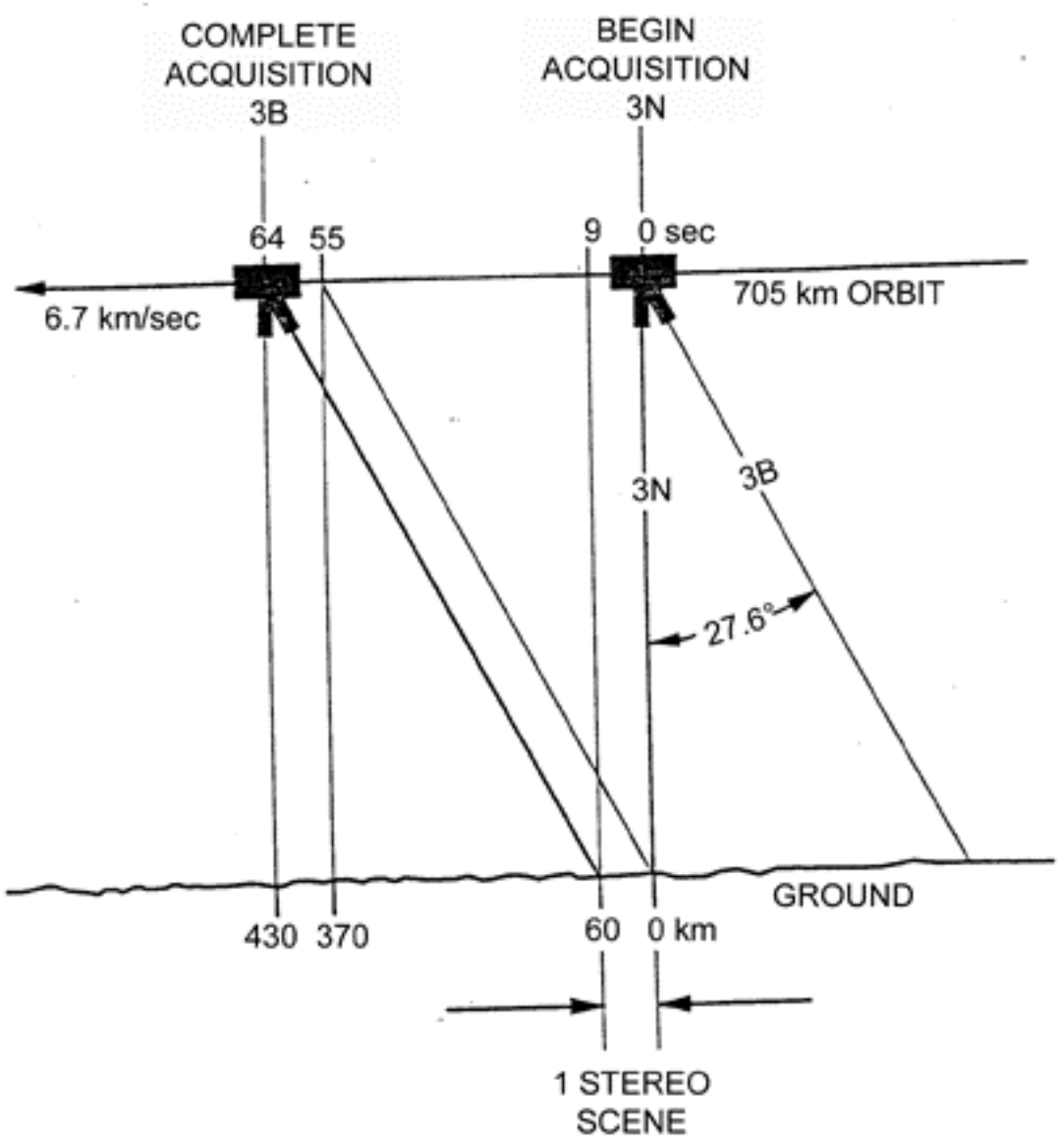

FIGURE 1.0-2. IMAGING GEOMETRY (APPROXIMATELY TO SCALE) AND DATA ACQUISITION TIMING FOR ASTER ALONG-TRACK STEREO.

Level 1 (Fujisada, 1998) (Figure 1.0-1), yielding over 1/2 million stereo pairs during the 5-1/2 year operational phase of the mission.

During the mission, ASTER will be capable of acquiring the 45,000 cloud-free, digital stereo pairs required to cover the land surface of the Earth. This conclusion is based on nine mission simulation results summarized in Figure 2.0-1. Without pointing, latitudinal coverage, based on the EOS AM-1 platform's orbital inclination of 98.2° is restricted to below 82°N and S.

Five of the simulations used to construct Figure 2.0-1 were conducted prior to 1994, during early mission planning. All five incorporated Willard's (1992) cloud climatology. Each simulation utilized a different value for acceptable percent cloud cover and window size for estimating cloud cover; these values ranged from 0% to 20% and 30 km to 90 km, respectively. These simulations also incorporated seasonal and latitude restrictions to assure optimal illumination. Specifically, winter solstice acquisitions were restricted to below 35°N latitude; spring equinox acquisitions were restricted to the region between 60°N and 45°S; summer solstice acquisitions were restricted to the region above 35°S; and autumnal equinox acquisitions were restricted to the region between 45°N and 60°N. Four other simulatons, conducted in late 1998 and early 1999, resulted in the lowest acquisition rate. These incorporated the additional requirement that all known EOS study targets be observed by ASTER multitemporally, whenever possible. They also incorporated extremely conservative mission operation scenarios and assumed low efficiency for the cloud prediction algorithm that is in the ASTER scheduler.

All nine simulations results, which vary substantially during mid years of the mission, show that acquisition of one cloud-free, stereo data set covering 80% of the land surface of the Earth is fairly certain by the end of the six year mission (Figure 2.0-1). These results are consistent with simulations reported for Stereosat (NASA, 1979) and Mapsat (Itek, 1981), as well as the actual results from Landsat reported by Welch and Marko (1981).

ASTER topographic data derived from this stereo dataset will augment that available from other sources (Figure 2.0-2; Table 2.0-1; see also Gittings, 1993, Wolf and Wingham, 1992, and Bohme, 1993). Absolute ASTER DEMs will be more accurate than National Imagery and Mapping Agency (NIMA; formerly Defense Mapping Agency, DMA) DTED-1 data, which has become the baseline prelaunch EOS digital topographic data set, even though they do not provide complete coverage of the land surface. The highest resolution global DEM data set available to the civil community is GTOPO30, with only 1 km posting and variable accuracy as bad as 2 km horizontal and ±650 m vertical (Table 2.0-1). The NIMA data set, with coverage outside the U.S. only available to the U.S. military community, provides only partial coverage of the land surface (Figure 2.0-2A) with 90 m posting, ±130 m horizontal and ±30 m vertical accuracy (Table 2.0-1). Existing land topographic mapping at a scale and accuracy equivalent to that provided by ASTER DEMs is similarly incomplete globally (Figure 2.0-2B).

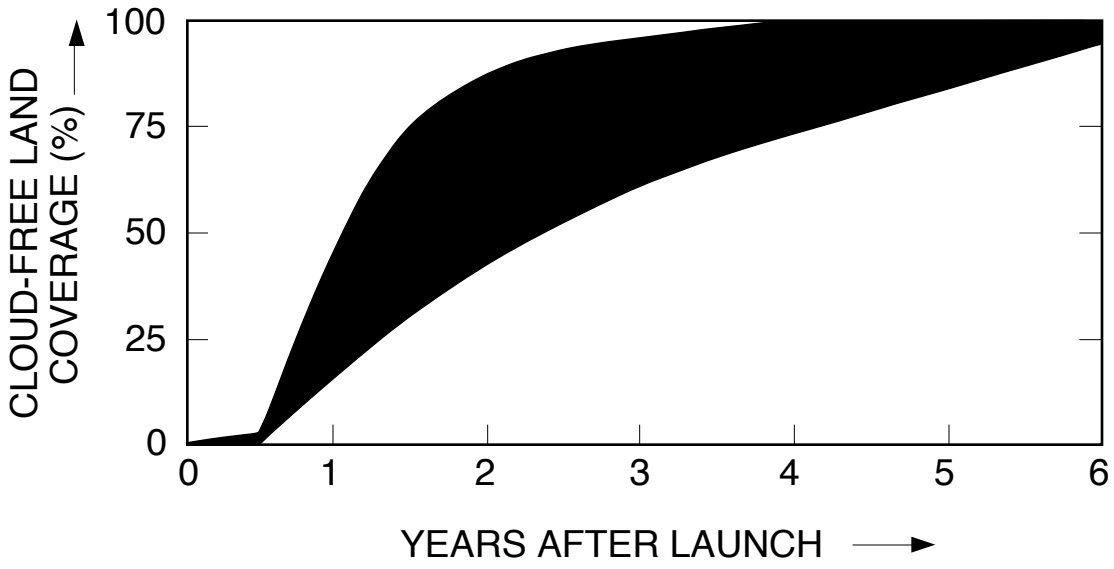

FIGURE 2.0-1. ACCUMULATED PERCENTAGES OF CLOUD-FREE GLOBAL LAND AREA COVERAGE BY ASTER STEREO FROM NINE CLOUD/MISSION PRIORITY SIMULATIONS. SEE TEXT FOR EXPLANATION.

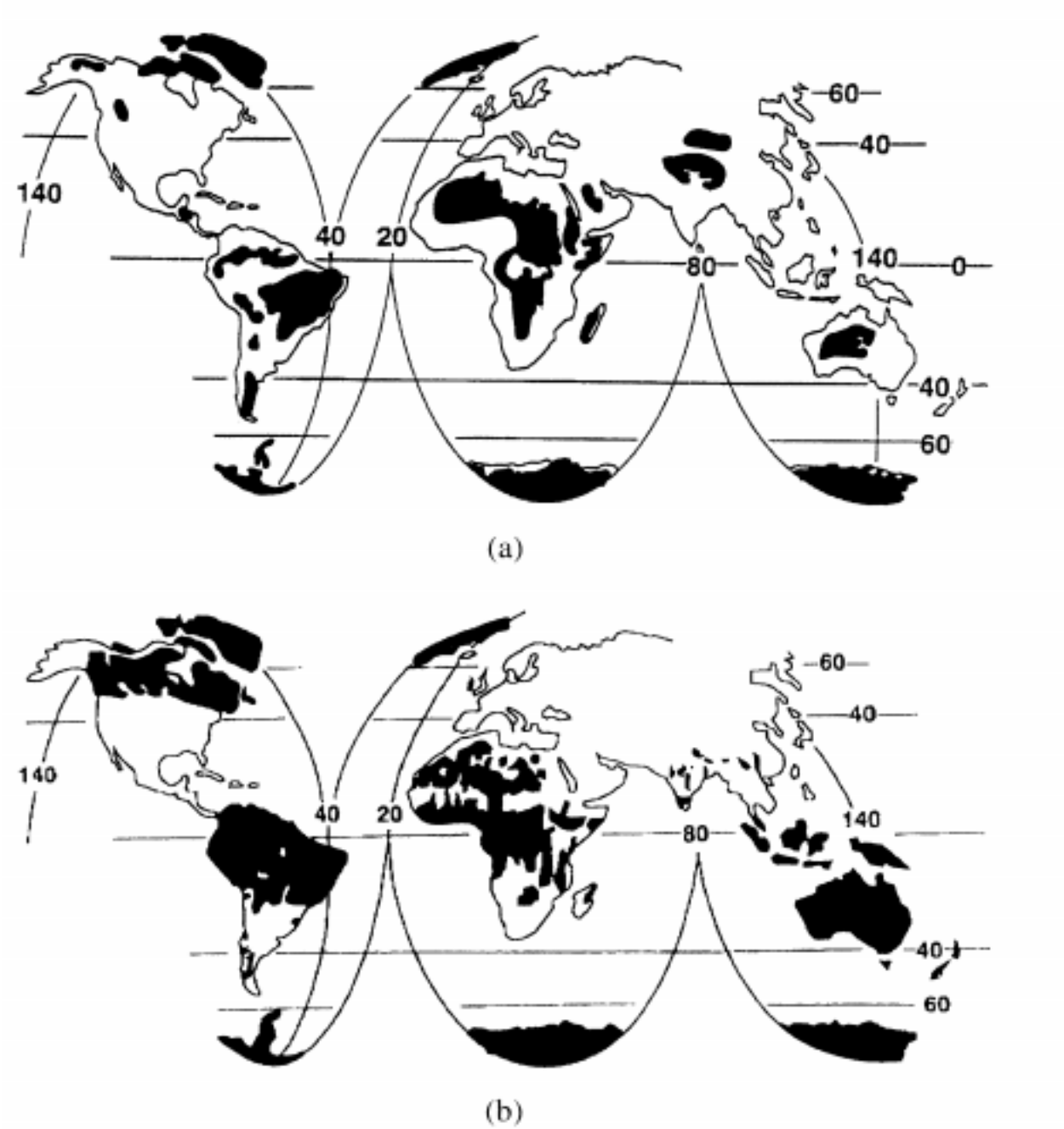

FIGURE 2.0-2. REGIONS OF THE WORLD WHERE ASTER DEMs WILL REPRESENT MAJOR CONTRIBUTIONS TO THE EXISTING TOPOGRAPHIC DATABASE. A. AREAS NOT COVERED (BLACK) BY NIMA DTED-1 DIGITAL ELEVATION DATA (TABLE 2.0-1). B. AREAS INADEQUATELY MAPPED AT SCALES OF 1:50,000 OR LARGER WITH RELIEF GREATER THAN 200 m. (COMPILED FROM MURPHY, 1968, AND BOHME, 1993).

TABLE 2.0-1. SPECIFICATIONS OF SELECTED, AVAILABLE DIGITAL ELEVATION MODELS (FROM GESCH, 1993). Only ETOP05 and GTOPO30 provide complete coverage of the Earth's land area.

Note: CE and LE refer to NMAS method for map accuracy assessment (Appendix 6-5).

PRODUCT	CELL SIZE	HORIZONTAL ACCURACY	VERTICAL ACCURACY
ETOP05	5' (10 km)	Not available	Not available
GTOPO30	30" (1 km)	2000 m (CE)*	±650 m (LE)*
NIMA DTED-1	3" (90 m)	130 m (CE)	±30 m (LE)
USGS 1/24 K DEMs	30 m	3 m (RMSE)	±7-15 m (RMSE)

* Based on least accurate input source data

The ASTER DEM capability is based on simple principles of geometry that were probably first documented by Pythagoras around 450 BC; and principles of photogrammetry that have been well understood and used routinely with stereo aerial photographs for nearly 70 years (von Gruber, 1930; American Society of Photogrammetry, 1952) (Figure 2.0-3). Application of these principles to digital satellite stereo data was inherent in the Stereosat (NASA, 1979; Welch and Marko, 1981) and Mapsat (Itek, 1981) missions which were first conceived 20 years ago. Practical implementation of digital photogrammetry has been demonstrated with results using data from numerous satellite systems (Table 2.0-2). The viability of a computer-automated procedure of stereo correlation for parallax difference/height measurement from digital stereoscopic data was first described and evaluated over 20 years ago (Appendix 6-2; Panton, 1978; Ackermann, 1984 and 1994), and has been demonstrated practically by commercial systems (Bolstad and Stowe, 1994, and Trinder et al., 1994) available for 10 years, even on personal computers (Gagnon et al., 1990, and Welch, 1989). Thus, it is evident that ASTER DEMs will be extremely valuable data products that can be produced using well understood principles and commercial, off-the-shelf software.

2.1 Experimental Objective

The objectives of the ASTER along-track stereo experiment during the six year mission are: 1) to acquire cloud free stereo coverage of 80% of the Earth's land surface between 82°N and 82°S; and 2) to produce, with commercial software, standard product DEMs at a rate of one per day at the Land DAAC.

ASTER's capacity for accomplishing objective 1) was described in Section 2.0. Objective 2) deserves further comment. The low, one-scene-per-day, production rate was selected for programmatic reasons by the EOS Senior Project Scientist based on review of three alternative production capabilities (Appendix 6-3). The production option selected will demonstrate that high quality ASTER DEMs, meeting the specifications in Table 3.0-1, can be produced using commercial software. We expect that the demonstrated methodologies likely will be adopted and refined by private industry and academic institutions. Individual scientists with appropriate computers and software will be able to create their own DEMs using ASTER Level 1 stereo images obtained from archives at the Land DAAC.

2.2 Historical Perspective

The ASTER stereo subsystem represents implementation of the Stereosat/ Mapsat concept to acquire global, along-track, digital stereo coverage of the land with a system designed specifically for photogrammetry. The only satellite systems that have provided digital, along-track stereo are the OPS system on the Japanese Earth Resources satellite (JERS-1) launched in 1993 (Nishidai, 1993), and the German MOMS system (Table 2.0-2). The JERS-1 system was designed primarily to deliver hard-copy stereo pictures for stereoscopic viewing and manual interpretation, and therefore has a base/height ratio (B/H) of only 0.3 (versus 0.6 for ASTER). Few published examples of OPS DEM results are available (GSI, 1993; Nishidai, 1993).

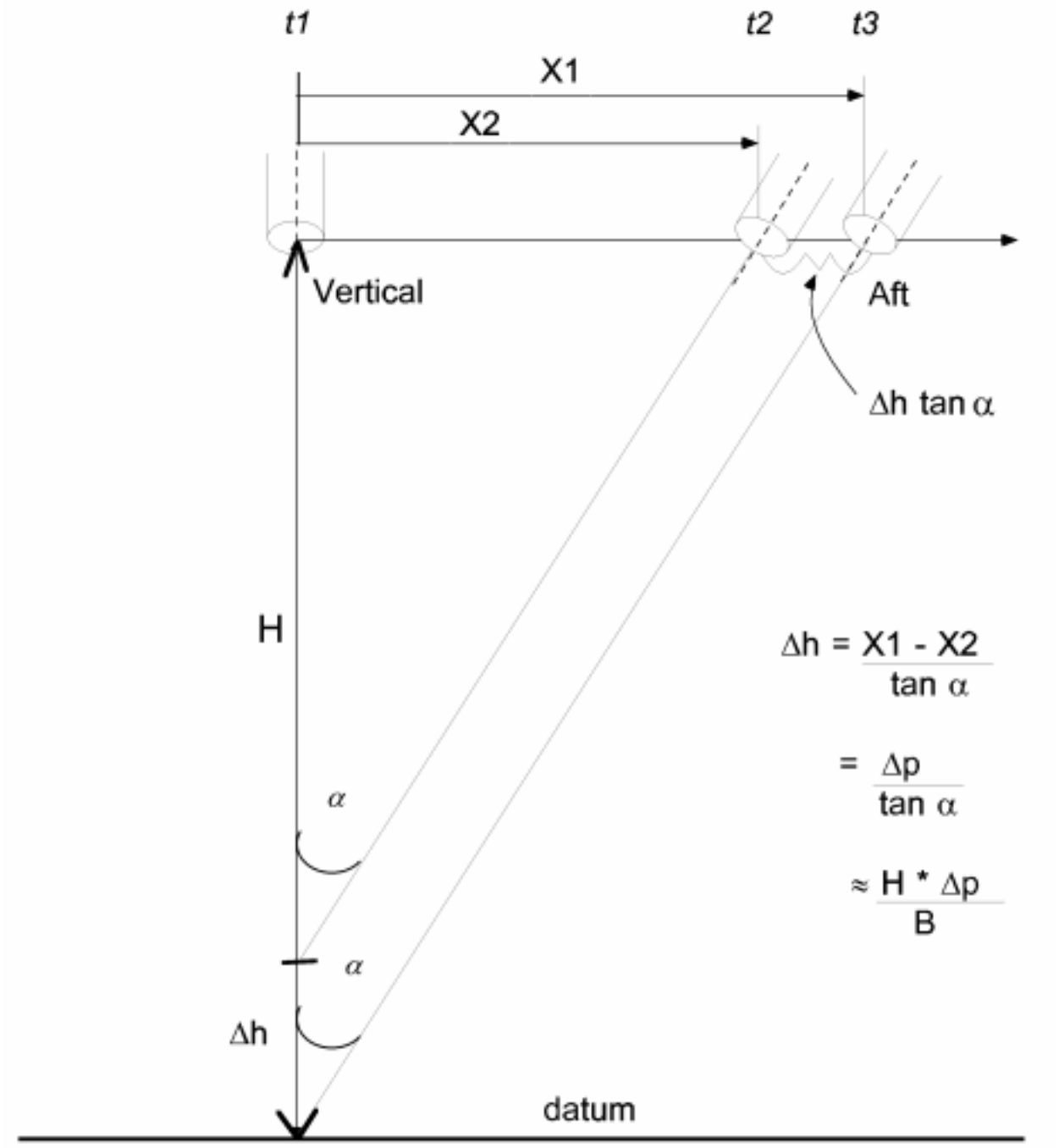

FIGURE 2.0-3. ALGORITHM FOR MEASURING HEIGHT (Δh) FROM PARALLAX DIFFERENCE (Δp) IN AN ASTER STEREO PAIR (NOT TO SCALE). BASE (B) IS EQUAL TO X_1. FOR THE NADIR (VERTICAL) AND AFT CAMERA CONFIGURATION, Δh IS RELATED TO THE CAMERA ORIENTATION ANGLE (α) AND THE TIME INTERVAL (Δt)REQUIRED TO RECORD BOTH THE TOP AND THE BOTTOM OF THE OBJECT. IN THE NADIR/AFT STEREOPAIR, Δt IS REPRESENTED BY $(X_1-X_2) = \Delta p$.

TABLE 2.0-2. SPECIFICATIONS OF SELECTED SPACE MISSIONS THAT PROVIDE OPTICAL STEREO DATA AND REPORTED RMSExyz OF DERIVED DEMs

Instrument/Mission	Agency/Year	Resolution Pixel Size (m)	Maximum Base/Height	RMSE-Accuracy (m) Z	RMSE-Accuracy (m) XY	Swath Width (km)
TM Landsat	NASA 1982-present	30	≤0.2*	40	30	185
MetricCamera Spacelab-1/STS-9	ESA/DFVLR 1983	~13**	~0.3	15	15	190
Large Format Camera STS-41C	NASA 1984	~8**	≤1.3	10	10	100
HRV SPOT	CNES 1986-present	10	≤1.0	10	10	60
MEOSS SROSS-II	DFVLR/ISRO 1988	80	1.0	~50	~30	255
LISS IRS	DS 1989-present	36	~0.1	~35	~15	148
MetricCamera Atlas-1	DFVLR/NASA 1991	5	≤0.6	~10	~10	190
Stereo-MOMS Spacelab-D2	DFVLR/NASA 1991/1992	5-10	1.0	~10	~10	32
OPS JERS	JAROS 1992-present	24	0.3	~35	~35	75
IRS-1C	DS 1994-present	6	1.0	~5	~5	75

* In regions where adjacent swaths have narrow sidelap
** Film

Examples of satellite systems that have provided either along track analog data or cross-track digital data also exist (Table 2.0-2). An example of the former is the Large Format Camera flown on only one Shuttle mission in 1984, and now mothballed. Examples of the latter include SPOT-1 through -3 systems, available since 1986. Also in Table 2.0-2 is the 6 m resolution, IRS-1C panchromatic system, launched in 1994 and providing cross-track digital stereo data with a B/H similar to SPOT.

The ASTER stereo subsystem design and DEM algorithm concept have benefited substantially from what has been learned from using Large Format Camera, Landsat, SPOT and IRS LISS stereo data for DEM generation (e.g., Al-Rousan and Petri, 1998; Al-Rousan et al., 1997 and 1998; Cheng and Toutin, 1998; Clavet et al., 1993; Derenyi and Newton, 1987; Ehlers and Welch, 1987; Rao et al., 1996; Research and Engineering Directorate, 1984; Theodossiou et al., 1990; Welch, 1989; Welch et al., 1985, 1990, and 1998).

2.3 Instrument Characteristics

Figure 1.0-2 depicts the ASTER along track stereo imaging geometry. The most important specifications of the ASTER stereo subsystem that govern the DEM generation capabilities, include: stereo geometry (one nadir viewing and one aft-viewing telescope, 27.6° off nadir); platform altitude of 705 km and ground speed of 6.7 km/sec; B/H of 0.6; IFOV of 15 m; bandpass of 0.76-0.86 micrometers (near infrared) in channel 3N (nadir) and 3B (aft), both with an MTF of 0.24; 9 seconds required to acquire a 60 x 60 km scene; 64 seconds required to acquire a stereo pair.

3.0 Algorithm Description and Implementation

A digital stereo correlation approach will be used to calculate parallax differences and derive DEMs from ASTER Level 1 stereo pairs. The mathematical concept of one approach to stereo correlation is described in Appendix 6-2; other mathematical treatments of equivalent procedures are provided by Ackermann (1984), Ehlers and Welch (1987), and Rao et al. (1996). ASTER standard product DEM production will use the PCI commercial off-the-shelf photogrammetric software to implement the procedure. This commercial system has been acquired and will operate at the Land Processes DAAC to produce the DEM standard data product at a rate of one scene per day, starting upon receipt of ASTER Level 1 stereo imagery, which will begin after initial engineering checkout, now planned to be completed 53 days after launch (Appendix 6-3).

Our plan for implementing this approach is summarized in Figure 3.0-1 and the DEM generation process is shown in Figure 3.0-2. It is very important to understand that the use of ASTER data in the DAAC environment requires some modification of the PCI software to achieve efficient processing of ASTER stereo data. Given the current knowledge of how ASTER stereo data will be supplied, it is anticipated that the DAAC will process the ASTER data on a scene-by-scene basis. For correlation and editing this is a reasonable approach. However, it may not be the best for the initial rectification/geocoding required before stereo correlation. As illustrated in Figure 3.2-1, GCPs will not be needed in every 60 x 60 km ASTER stereo pair to produce an

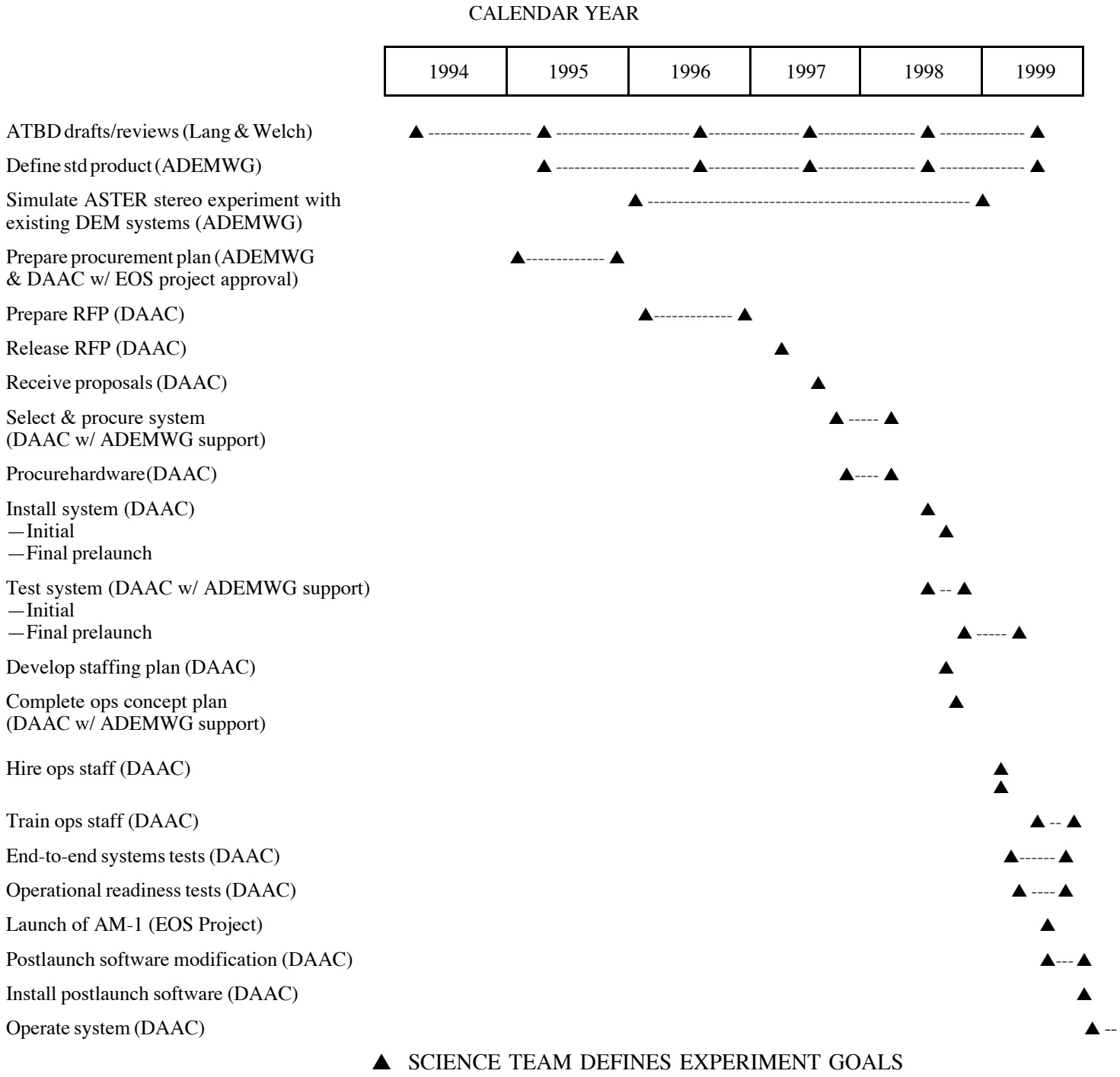

FIGURE 3.0-1. IMPLEMENTATION SCHEDULE (AND RESPONSIBILITIES) FOR ACQUIRING, TESTING AND OPERATING ASTER DEM GENERATION SYSTEM AT THE LAND DAAC (ASSUMING JULY, 1999 LAUNCH).

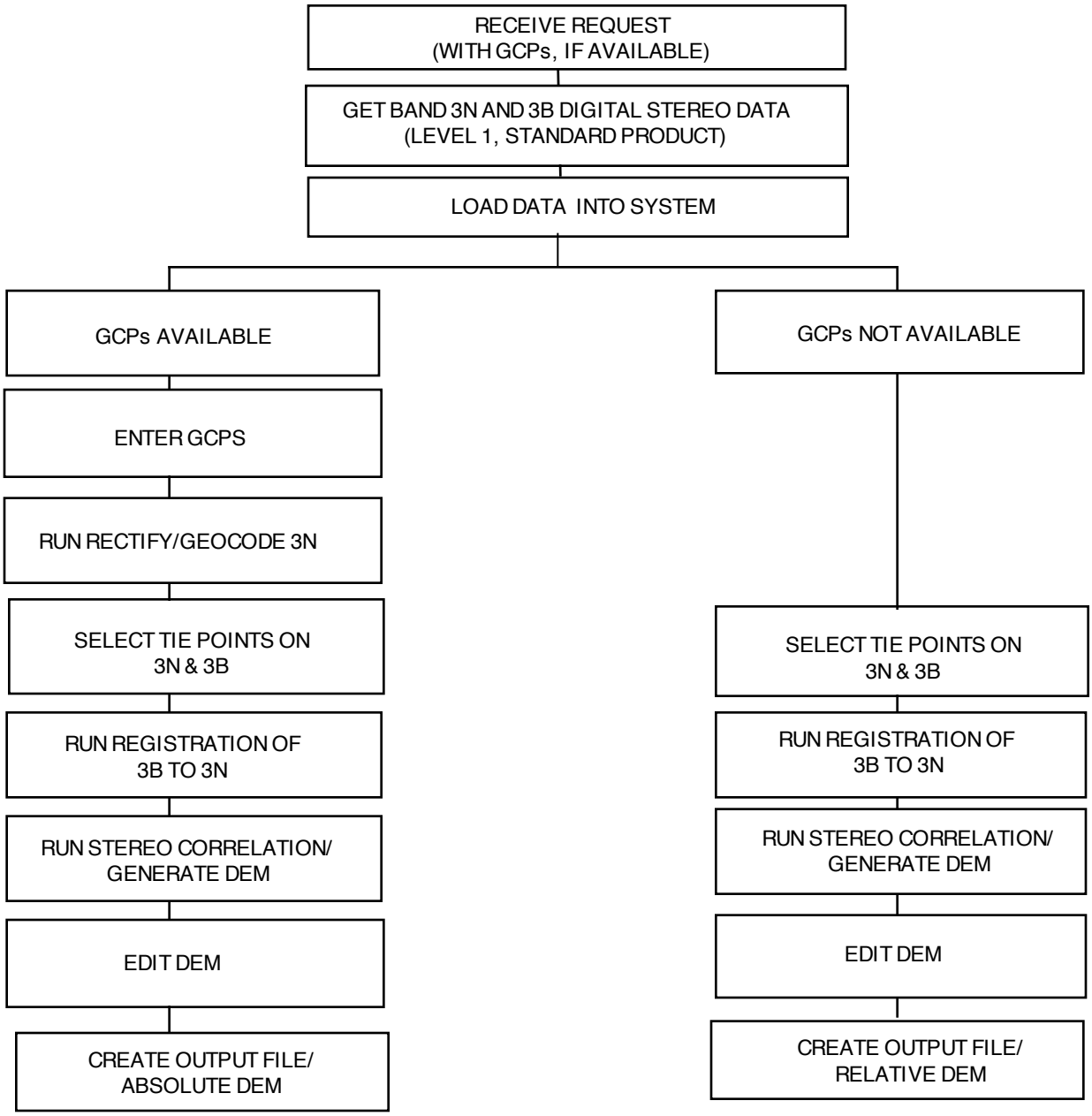

FIGURE 3.0-2. FLOW CHART SUMMARIZING STANDARD PRODUCT DEM GENERATION PROCESS (SUBJECT TO MODIFICATION AS DISCUSSED IN TEXT)

absolute DEM. This approach of block adjustment to extend the effect of ground control is very valuable. The system should be flexible enough to handle blocks of ASTER stereo scenes. Alternatively, the control selection/rectification processing can be accomplished simultaneously for groups of scenes from the same swath and/or adjacent swaths, with correlation and editing performed on an individual scene basis in the DEM generation system. We will also investigate stereo correlation on a swath basis, with final editing and output on a scene basis. The effects of the different approaches on accuracy and quality (i.e., edge matching of adjacent DEMs) also will be characterized by the DAAC. This work will continue until the system is operational at launch, which is now expected in July, 1999.

The PCI system to be used for ASTER DEM generation has the capability to perform simultaneous adjustment of several scenes from different swaths (block adjustment), several scenes from a single swath (swath adjustment), or scene-by-scene adjustment. As noted above, the advantage of simultaneously processing large areas is that the number of ground control points required per unit area can be reduced. Also, the problem of edge joins is mitigated. Due to the large number of computations and processing times, the correlation and editing will be performed on a scene-by-scene basis. Since the imagery will be introduced into the system in units of one scene, the actual process will be a “strip adjustment” (several individual scenes simultaneously adjusted) rather than a true “swath adjustment” (a single long, contiguous strip of data adjusted as one unit). This will have little, if any, measurable affect on the efficiency of the process or accuracy of the output DEM.

The process for generating DEMs using the PCI or other commercial systems is outlined in Figure 3.0-2. Table 3.0-1 shows specifications of the standard ASTER DEM data product. The process depicted in Figure 3.0-2 shows that the generation of DEMs requires the construction of a stereo pair by registering two images of the same ground area recorded from different positions in space. In the stereo pair, any positional differences parallel to the direction of satellite travel (parallax differences, Δp) are attributed to displacements caused by relief (Figure 2.0-3). Relative ground elevations are determined by measuring Δp in the registered images. The Δp are converted to relative or absolute elevations (Z-coordinates) in a subsequent step.

The ASTER aft-camera image (band 3B) can be registered to the nadir (band 3N) reference image by establishing transformation equations for conjugate image locations. The result of the transformation computation is a set of coefficients that define the relationship between both images of the stereo pair. In the process of developing DEMs, it is important to minimize resampling operations to retain the original image data quality and to reduce disk transfer time and storage requirements. The transformation equations which register the 3B to the nadir 3N images can be implemented using image segments in the correlation process. No resampling is required at this stage.

TABLE 3.0-1. DEFINITION/SPECIFICATIONS FOR STANDARD ASTER DEM DATA PRODUCT(S)

UNIT OF COVERAGE: 60 km x 60 km ASTER scene

FORMAT: Data consist of a regular array of elevations (in meters) referenced to either the lowest elevation in the scene ("relative DEM") or to mean sea level ("absolute DEM") and projected in the Universal Transverse Mercator (UTM) coordinate system.

RESOLUTION:
1. X-Y; 30 m (posting)
2. Z; 1 m (smallest increment)

PRODUCT NAME	# OF GCPs (MINIMUM)	GCP (RMSExyz) ACCURACY	DEM (RMSExyz) ACCURACY
Relative DEM	0	N/A	10 - 30 m*
Absolute DEM	1	15 - 30 m	15 - 50 m**
Absolute DEM	4	5 - 15 m	7 - 30 m**

* Z values referred to lowest elevation pixel in the DEM, and "accuracy" is relative to this pixel.
** Z values referred to absolute vertical datum (mean sea level)

Because of inadequate pointing and ephemeris information for use with 15 m ASTER pixels, absolute DEMs must be referenced to a map coordinate system using ground control points (GCPs). This is because platform pointing knowledge for the EOS AM-1 platform is expected to be about 300 m in X and Y, according to O'Neill and Dowman (1993); and the X-Y accuracy of ASTER Level 1 data should be about 50 m according to Fujisada (1998). GCPs are features that are distinct and identifiable on the image, and for which the X, Y and Z coordinates are known (Appendix 6-4). The accuracy requirements for GCPs is shown in Table 3.0-1. The coordinates of all ASTER GCPs will be recorded in the Universal Transverse Mercator (UTM) coordinate system referenced to the World Geodetic System of 1984 (WGS84) ellipsoid for foreign areas, and to the North American Datum of 1983 (NAD83) for areas within the United States and Canada (Snyder, 1982; Pearson, 1977). GCP information, including ASTER input image line and sample coordinates, will be provided by the customer. These image coordinates of the GCPs in conjunction with their UTM map coordinates will permit the development of transformation equations needed to register the stereo images and eventually geodetically rectify them to the Earth's surface.

The stereo correlation procedure is statistical and is utilized to derive automatically a digital elevation model (DEM) from the registered stereo pair (Ackerman, 1984; Ehlers and Welch, 1987; Rao et al., 1996; Welch, 1989; Welch et al., 1998). It is a complex task requiring large numbers of floating point computations on 16 million pixels in each ASTER image forming the stereo pair.

After transformation coefficients have been calculated, the band 3N and the band 3B full scene images must be "matched" to establish Δp values. To accomplish this, a correlation window of specified size (e.g., 11 x 11 pixels), defined prior to initiating the correlation procedure, is automatically centered over a 15 m pixel in the band 3N image. The area on the band 3B image within which the conjugate pixel is located is defined by a search window sized to account for the maximum possible image displacements due to terrain relief. The correlation window is then moved pixel-by-pixel across the search window and the correlation coefficient computed at every pixel location. The pixel location at which the correlation coefficient reaches a maximum is considered to be the "match point". The difference in pixel location (in the conjugate images) parallel to the direction of satellite motion is the Δp value, and is proportional to the terrain elevation relative to the vertical datum (Figure 2.0-3). This procedure is systematically repeated across image space.

Although it is not necessary to determine Δp values for every image pixel, the matching process must be operated on a per pixel basis. This optimizes reliability of the correlation coefficient and accounts for high frequency terrain variations. Subpixel Δp values can be achieved by interpolation. Early ADEMWG simulation results on a single Pentium-based, PC workstation indicate a performance rate of 50 to 200 elevation posts per second (the wide range is due to variations in workstation performance, algorithmic design, image quality and relief). Based on this example, 6 to 22 hours of computation time will be required to generate a DEM with 30 m spacing from an ASTER stereo pair using commercial systems such as those described by Welch (1989) and Trinder et al. (1994). Based on simulations and data supplied by PCI as part of their response to the request for proposals for commercial system

selection, the actual ASTER DEM workstation should perform the autocorrelation of one ASTER stereoscopic image pair in about three to six hours, depending in the variables noted above.

Upon completion of the correlation step, all pixels must be geodetically rectified to the UTM coordinate system. This rectification process includes scaling, translation, rotation, warping and resampling of the data pixels.

For some pixels, the correlation will fail or produce inadequate results in a typical scene. Therefore, completion of the DEM generation process requires a final editing step using a series of batch and interactive processes provided by the PCI software. It has been shown that with these standard image processing routines, the DEM can be filtered to correct for spikes and outliers in the dataset (Giles and Franklin, 1996; Kok et al., 1987).

The process described here may differ somewhat from that of the PCI system as finally used operationally by the DAAC. For instance, Figure 3.0-2 shows locating of GCPs on the nadir image, followed by rectification, and then tie point selection between the nadir and aft images to accomplish registration. An alternative approach is simultaneous rectification and registration of the nadir and aft images by locating the GCPs on both images at the same time; so that they serve as tie points for the initial image 3N and 3B registration as well.

The PCI software performs the rectification and registration processes simultaneously. The output from the system autocorrelation process is in ground space. Consequently any required editing will be conducted in ground space. These differences from the generalized processing flow shown in Figure 3.0-2 will have little or no effect on the efficiency or accuracy of the overall process.

Another example of the potential difference between the Figure 3.0-2 process and how the PCI system will be used operationally is the stage at which image correlation occurs and Δp values are converted to elevations. Correlation/editing can be performed in image space and then Δp values are converted to elevations and rectified into ground/map space, or all correlation and editing can be performed in ground/map space.

The PCI software will make use of the ephemeris and attitude information recorded in the ASTER metadata. These ephemeris and attitude data are used to calculate the transformation coefficients between the map and image coordinate systems. Such an approach greatly reduces the number of ground control points needed to create a DEM. Scientists from the Geographical Survey Institute in Japan, for example, have successfully used ephermeris and attitude data in conjunction with widely spaced GCPs to generate absolute DEMs from JERS-1 stereo image data (GSI, 1993). Although the RMSExyz values of these DEMs as evaluated against GCPs withheld from the adjustment procedure degraded by about a factor of two compared to DEMs produced with full ground control, this approach does provide a means for producing DEMs to sufficient accuracies for creating orthoimage products or for topographic correction of other EOS data products in areas without GCPs. It is important to note that the “relative accuracy” of the Z values will be correct to within the threshold of measurement, i.e., approximately ±20 m. Thus, DEMs with this sort of relative

accuracy can be used effectively to aid geomorphic, geologic and vegetation studies in remote areas of rugged terrain.

An important topic of ongoing research and development is how to reduce the requirement for human intervention in the DEM generation process. The stereo correlation process is highly automated, but based on our experience manual editing remains a necessary and time-consuming task. The degree to which editing is required depends greatly on the nature of the stereo imagery. The only existing, routinely available satellite sources of optical stereo imagery is SPOT, and the temporal differences in the images due to its repeat pass cross-track stereo collection mode usually results in a need for significant manual editing. Because ASTER stereo pairs will be acquired along-track and nearly simultaneously (Figure 1.0-2), these large temporal differences will not be present. Our ongoing experiments with JERS-1 stereo data will provide some insight into improvements resulting from the along-track stereo mode. However, there will always be areas of clouds, shadows, water, and low contrast ground cover where correlation will fail, or be unreliable, and operator intervention is required. Research into ways to reduce or even eliminate manual editing will be a continuing activity at the Land DAAC DEM production facility throughout the mission.

Another area in which improvements would reduce the need for operator intervention is in the selection of ground control/tie points. Methods for automating, and thereby speeding up, the process would result in significant enhancement of the DEM generation process.

The use of ancillary topographic information, such as geomorphic feature data (streams, ridgelines, lake shorelines, spot heights, local depressions, etc.) derived from other sources as input to the DEM correlation and editing processes have sometimes been used in DEM processing. The current version of PCI software at the Land DAAC does not have the capability to utilize these ancillary sources of information to constrain the autocorrelation process or to support the editing. Although this could be a valuable tool for the generation of more accurate DEMs, it was not given a high priority in the procurement because it has been our experience that the ancillary digital data, such as the examples noted in the preceeding paragraph, usually become available after, not before, a DEM is produced.

3.1 Accuracy, Precision and Resolution: Error Estimates

Here we first provide a description of the parameters of interest in characterizing accuracy, precision, and resolution of ASTER DEMs. We then describe how we estimate values for these parameters for ASTER DEMs.

Planimetric and elevation error standards have existed for paper cartographic products (maps) for over half a century (Bureau of the Budget, 1947, and Appendix 6-5). With the advent of digital cartographic data, these standards, based on map measurements and hence map-scale dependent, have been refined to incorporate statistically based measurements of accuracy. Commonly used statistical measures of map accuracy are the Root Mean Square Error (RMSE) in XY (planimetry) and Z (elevation). RMSE is defined in Appendix 6-6; an RMSE-based map accuracy standard is provided in Appendix 6-7.

Reported accuracies for GTOPO30 and NIMA DTED-1 data use the Bureau of the Budget (1947) method, and the USGS 1:24,000 scale DEMs use the RMSE method (Table 2.0-1). We will use the RMSE measure for ASTER DEM accuracy assessment. Integrated results from geometric analyses, analogy with other satellite systems and simulations of ASTER data have been used to estimate RMSExyz for ASTER DEMs (Table 3.0-1). Comparison of Table 3.0-1 to Table 2.0-1 shows that absolute ASTER DEMs will be more accurate than DTED-1 DEMs which are the baselilne prelaunch EOS digital topographic data, but do not provide complete global coverage of the land (Figure 2.0-2B).

A simple geometry-based photogrammetric rule that is applicable to assessment of ASTER DEM accuracy is:

$$\Delta h = \frac{H\Delta p}{B} \qquad \text{(Welch 1989)}$$

where H/B is the inverse of the B/H ratio (in the case of ASTER 1.0/0.6 or 1.7), and Δp is the difference in parallax (xy displacement) of a point in the two images forming the stereo pair. Assuming Δp correlation errors in the range of 0.5 to 1.0 pixels (7-15 m), Δh errors (RMSEz) would be in the ±12 m to ±26 m range. This estimate accounts for typical errors due to correlation alone. It does not account for the fact that knowledge of imaging geometry is imperfect. According to Arai's (1992) accuracy assessment that incorporated available information about ASTER system geometry and a more generalized error analysis for high resolution satellite photogrammetry by Li (1998) GCP and correlation errors are the primary factors affecting DEM accuracy. These analyses show that with GCPs with RMSExyz of about ±8 m, resulting ASTER DEMs would have RMSEx of ±15 m, RMSEy of ±11 m and RMSEz better than ±46 m. These conservative results are similar to those obtained in equivalent analyses independently by O'Neill and Dowman (1993). More recently, Tokiunaga and Hara (1996) and Tokunaga et al. (1996) estimated that ASTER RMSEz values of ±12.5 m should be possible.

Table 2.0-2 includes actual DEM accuracies obtained using stereo data from other satellite systems. In all cases RMSE values obtained using actual data are better than would have been expected based on prelaunch information alone. Overall, actual results reported in Table 2.0-2 show that, in spite of a wide range of platform and system characteristics, RMSExyz approximately equivalent to system instantaneous field of view (or pixel size) should be expected. This expectation is also supported by results from our analyses of DEMs generated from simulated ASTER data sets. We used SPOT stereo data with the ASTER B/H of 0.6. SPOT data were resampled to 15 m resolution ASTER pixels. Error assessment was accomplished by subtracting the ASTER-simulated Z values on a pixel by pixel basis from those on an existing DEM of known accuracy. All differences were assumed to result from errors in the simulated ASTER DEM. Figure 3.1-1 displays these results from the area covered by the Huntsville, Alabama, USGS 7-1/2 minute digital elevation model. Posting of ASTER-simulated Z values was 30 m to match that of the USGS model. The resulting RMSEz is ±13 m. It should be noted that the USGS DEM has an RMSEz of ±7-15 m, based on specifications. Equivalent results were obtained in a similar analysis conducted independently over Kiso-Komagatake, Japan, by Arai (1992). Other independent, SPOT-

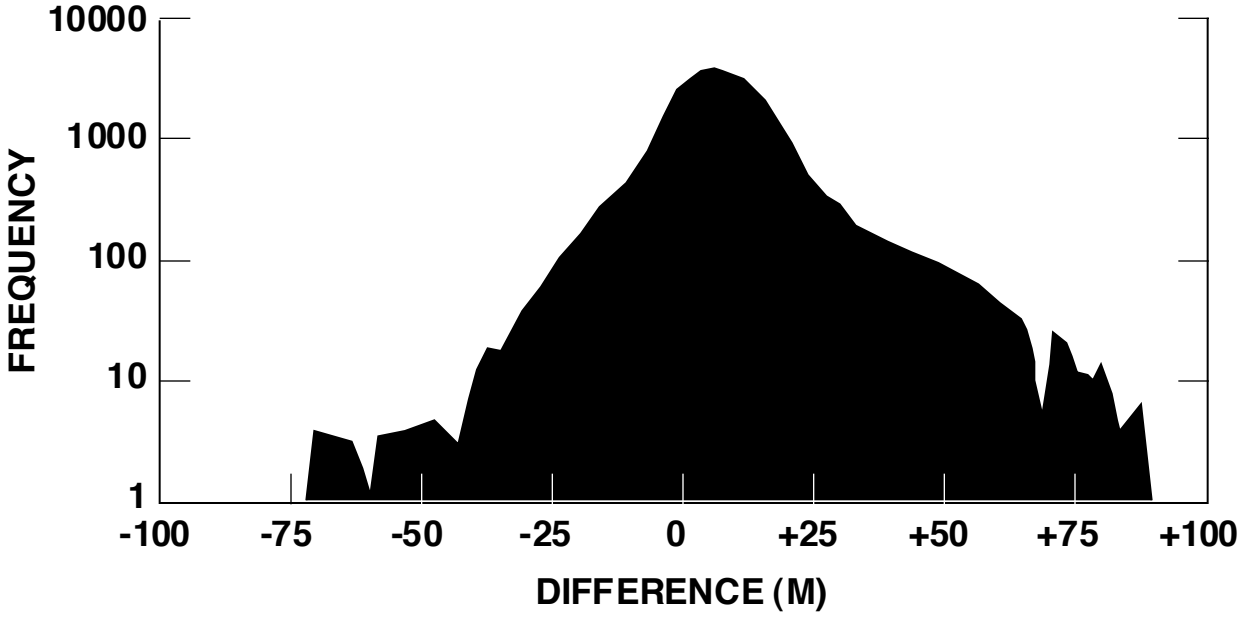

FIGURE 3.1-1. HISTOGRAM OF ELEVATION DIFFERENCES BETWEEN USGS 7.5 MINUTE DEM (RMSEz 7-15 m) COVERING THE HUNTSVILLE, ALABAMA, QUADRANGLE AND THE CORRESPONDING ASTER-SIMULATED DEM DERIVED FROM SPOT DATA RESAMPLED TO 15 m.

based ASTER simulations by Dowman and Neto (1994) yielded RMSE of approximately ±13 m (XY) and ±26 m (Z) for a site in SW France; and by Giles and Franklin (1996) yielded RMSExyz of ±22 m.

As pointed out by Gesch (1993), Bolstad and Stowe (1994), and Ackermann (1994) RMSExyz alone is an insufficient measure of DEM data quality for those who use the DEM data for scientific applications. Other parameters include: 1) the spacing of the DEM grid in XY (also referred to as posting, pixel size or XY precision), 2) the resolution of the DEM in Z (also referred to as Z precision, and numerically the smallest Z increment), 3) slope measurement accuracy (a derived value, dependent on RMSEz as well as the measurement distance in XY), and 4) equivalent map scale based on map accuracy standards. Figure 3.1-2 depicts the relationship of three of these parameters diagrammatically. Figure 3.1-2C requires additional comment. For absolute ASTER DEMs (Table 3.0-1) data consist of a regular array of elevations, Z values, which are referenced to mean sea level. As noted by the Topographic Science Working Group (1988), over 18 mean sea level datums are used by the various cartographic agencies that produce topographic maps worldwide (Figure 3.1-3). Errors in these datums would be introduced into ASTER DEMs through GCPs. The Topographic Science Working Group considered this sort of problem sufficient to fatally compromise any approach to global topographic mapping that required the use of GCPs. Fortunately, this concern is unfounded. According to an inhouse study by the U.S. National Geodetic Survey (Dave Zykowski, 1994, personal communications) the RMSEz of all of these datums world-wide is 1.5 m over a total range of error of only 3 m. Errors of this magnitude are inconsequential for the 1:50,000—1:250,000 scale map accuracy requirements of an ASTER-class DEM, and would even be inconsequential for 1:24,000 scale mapping.

As summarized in Table 3.0-1, posting in ASTER DEMs will be 30 m; vertical resolution will be 1 m. Table 3.1-1 shows that, based on expected RMSEz values for ASTER DEMs (±10-50 m, according to Table 3.0-1), slope accuracies of 5° should be obtainable over measurement distances in the 100 m to 500 m and longer range.

The cartographic value of DEM data can be measured by determining equivalent map scale. This can be done by considering RMSExyz values as well as the XY posting and Z resolution in the context of the Appendices 6-5 and 6-7 map accuracy standards. Welch and Marko (1981) quantified these relationships (Table 3.1-2). We estimate conservatively that ASTER DEMs will be generally useful at mapping scales in the 1:100,000 to 1:250,000 range. In some cases, ASTER DEMs will be of sufficient quality for 1:50,000 scale mapping.

3.2 Practical Considerations

Our basic DEM processing concept requires that one or more GCPs per scene be provided by the requestor if an absolute DEM is requested (Table 3.0-1). The requestor will provide the line and sample pixel locations of GCPs on the ASTER Level 1 band 3N and 3B images that will be used to produce the DEM.

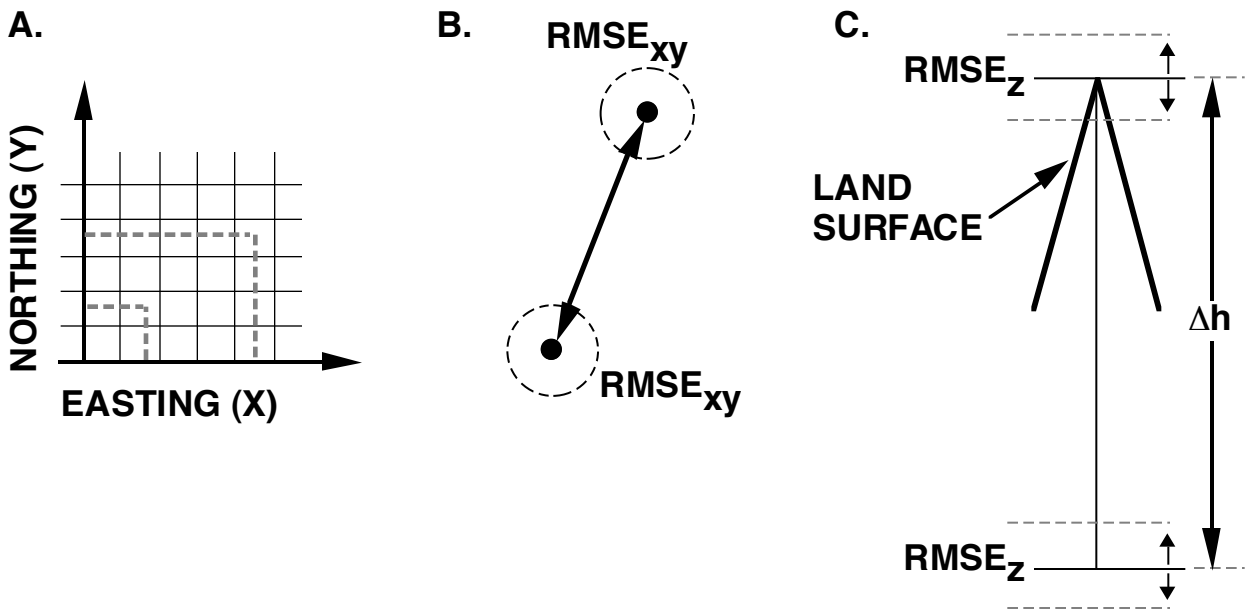

FIGURE 3.1-2. ILLUSTRATION OF RELATIONSHIP OF PLANIMETRIC AND HEIGHTING RESOLUTION AND ACCURACY

A. REGULAR POSTING SCHEME FOR DEM RASTER DATA.

B. MAP VIEW (XY, PLANIMETRIC) ACCURACY.

C. CROSS SECTION VIEW (Z, HEIGHTING/VERTICAL) ACCURACY.

SEE TEXT FOR EXPLANATION.

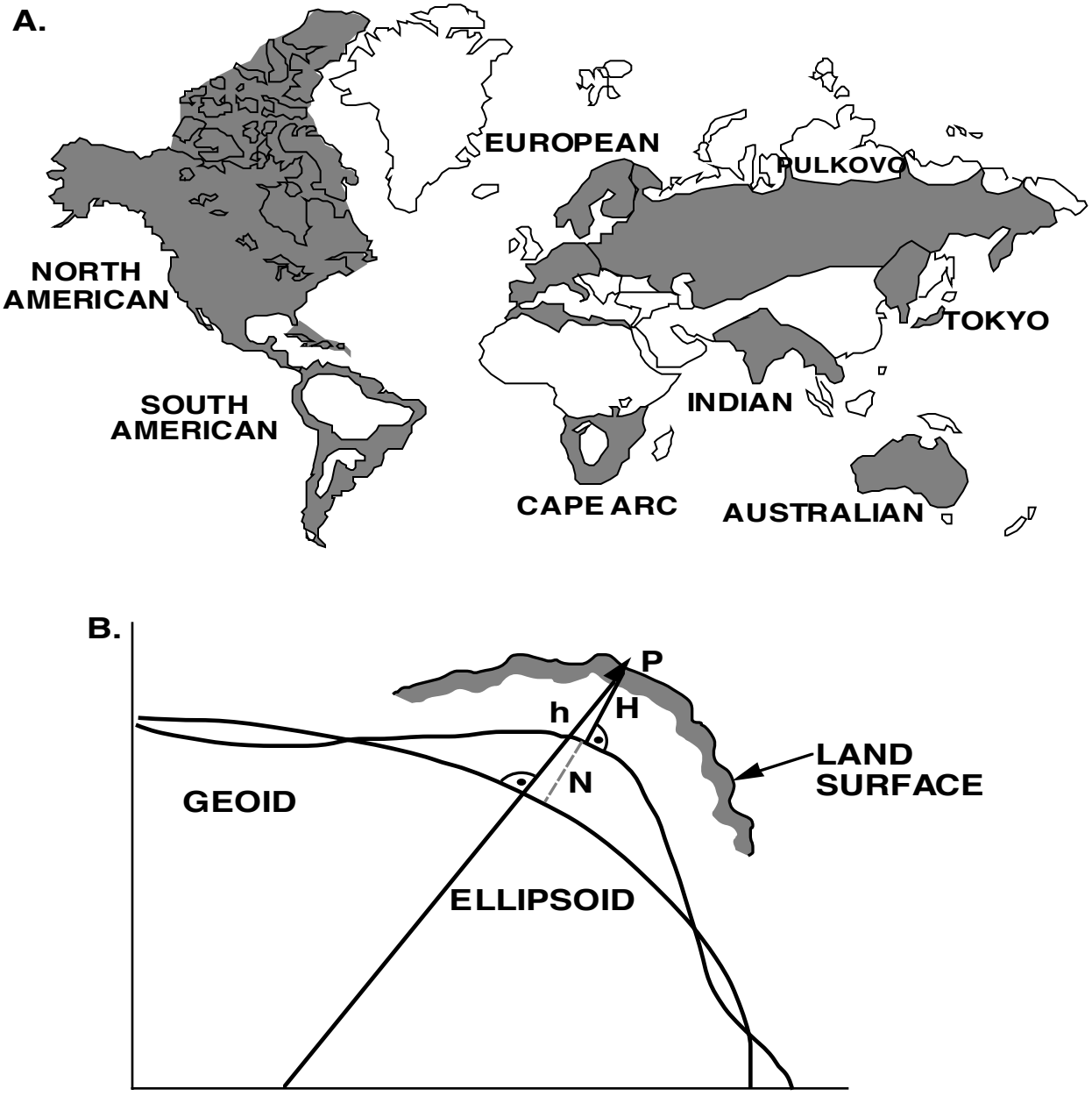

FIGURE 3.1-3. THE VERTICAL DATUM ISSUE.

A. MAP SHOWING MAJOR BLOCKS IN WHICH DIFFERENT VERTICAL (MEAN SEA LEVEL) DATUMS ARE USED (FROM TOPOGRAPHIC SCIENCE WORKING GROUP, 1988).

B. DIAGRAMMATIC CROSS SECTION VIEW ILLUSTRATING THE RELATIONSHIP OF THE GEOID, ELLIPSOID AND GROUND SURFACE (FROM SCHERRER, 1985). P IS A POINT ON THE EARTH'S SURFACE; N IS THE GEOID SEPARATION; h IS THE ELLIPSOIDAL HEIGHT; H IS THE HEIGHT ABOVE THE GEOID. H IS MOST USUALLY KNOWN AS THE HEIGHT ABOVE MEAN SEA LEVEL, AND IS USED FOR MAP DESIGNATION OF ELEVATION. THE RMSEz VARIATION OF THE MEAN SEA LEVEL DATUMS USED IN ALL THE AREAS SHOWN ON A. IS ONLY 1.5 m GLOBALLY.

TABLE 3.1-1. RELATIONSHIP OF MAP DISTANCE (CELL SIZE = POSTING) AND HEIGHT ERROR THAT RESULT IN SLOPE MEASUREMENT ERROR OF 5°.

Note: ASTER DEMs should provide slope measurement errors less than 5° over map distances of about 100 m and greater.

DEM CELLSIZE/LENGTH OF HORIZONTAL MEASUREMENT	CELL HEIGHT ERROR CAUSING 5° SLOPE ERROR (APPROXIMATE)
30 m	2.6 m
50 m	4.5 m
100 m	8.7 m
200 m	17.5 m
500 m	43.7 m
1000 m	87.0 m

TABLE 3.1-2. EQUIVALENT RMSE ACCURACY REQUIREMENTS FOR TOPOGRAPHIC DATA THAT MEET NATIONAL MAP ACCURACY STANDARDS (APPENDIX 6-5). (AFTER WELCH AND MARKO, 1981).

Map scale	RMSExy (m)	RMSEz (m)*
1:500,000	150	30
1:250,000	75	15-30
1:100,000	30	6-15
1:50,000	15	6
1:25,000	7.5	3

* Based on spot height measurements and contour intervals used for typical topographic maps of the specified scales.

Depending upon their distribution, however, fewer GCPs will be needed, on-average, per scene. A few examples of practical situations that lead to this conclusion are illustrated in Figure 3.2-1. For example, Dowman and Neto (1994) show that for 3000 km long strips of ASTER data, as few as six GCPs should provide sufficient control to meet accuracies specified in Table 3.0-1. Taking advantage of this approach to GCP economy, however, requires that an accessible archive of all GCPs submitted during the mission be maintained (Appendix 6-4).

Other practical considerations related to GCPs include their characteristics, potential sources, and cost. To be of use in the processing scheme portrayed in Figure 3.0-1, and in addition to RMSExyz specifications that are shown in Table 3.0-1, a GCP must be locatable at the 15 m pixel level on an ASTER Level 1 Band 3N image. We therefore require that the ASTER absolute DEM requestor provides the line and sample locations of all GCPs on the ASTER Level1 Band 3N and 3B input images.

As described by Clavet et al. (1993) and Kardoulas et al. (1996), sources for GCPs for use in satellite photogrammetry include existing topographic maps, photogrammetric triangulation from aerial photographic surveys, and global positioning system (GPS) data. Topographic map sources at 1:25,000 scale will satisfy our most stringent GCP accuracy requirement. In most cases, 1:100,000 or 1:50,000 scale sources will probably provide sufficient accuracy (Table 3.0-1). GCPs with RMSExyz better than 15 m can be obtained from 1:50,000 scale maps that meet National Map Accuracy Standards (Appendix 6-5 and Table 3.1-2); RMSExyz of 15-30 m can be obtained from 1:100,000 scale maps. As documented by Bohme (1993), such data exist for much of the land area of the world (Figure 2.0-2.3). As determined by Clavet et al. (1993), differential GPS measurements, using inexpensive, off-the-shelf, hand-held receivers, provide GCP data that satisfy the better than 15 m RMSExyz ASTER requirement.

Selection of the 30 m posting for ASTER DEMs (Table 3.0-1) is based on both expected RMSExy as well as practical consideration. Although successful stereo correlation of all 15 m ASTER pixels may be accomplished in exceptional situations, normally correlation failures will occur. The 30 m posting requires successful stereo correlation of one, 15 m ASTER pixel out of every four (a 25% or greater success rate) and distributed evenly planimetricly. In situations where a lower success rate is accomplished, no ASTER DEM will be produced. The criteria for a “successful” correlation will be clearly defined, as will an “even planimetric distribution” of successful correlations. This will be reported as part of the Quality Assurance metadata (see 3.2.3 below). This data layer will be useful to ASTER DEM users for characterizing the spatial distribution of successful or failed correlations, and for identifying areas in a particular DEM where accuracy should be verified.

3.2.1 Numerical Computation Considerations

Assessing accurately the computational needs and costs for ASTER DEM production requires information about the exact number of ASTER DEMs that will be produced during the mission. Based on a study of the costs/benefits of three production rate options (Appendix 6-3), the EOS Project selected the one scene/day

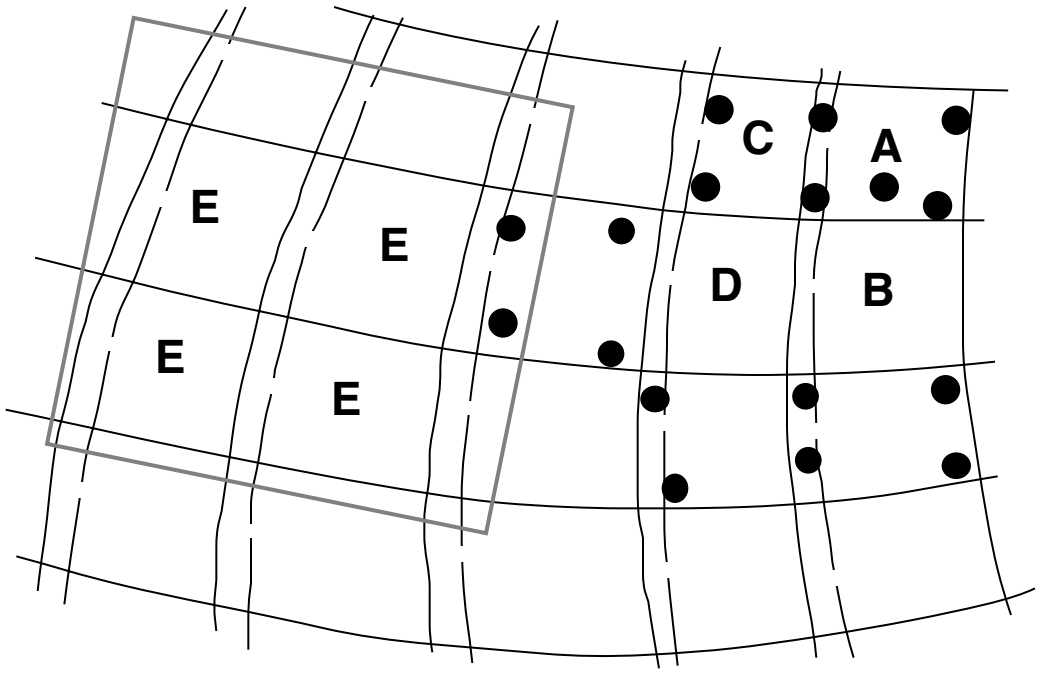

FIGURE 3.2-1. DIAGRAM ILLUSTRATING THE FACT THAT UNDER ACTUAL CONDITIONS, THE NOMINAL BASELINE REQUIREMENT OF FOUR OR MORE GCPs/ ASTER STEREO PAIR FOR PRODUCTION OF ABSOLUTE DEMs (TABLE 3.0-1) IS EXCESSIVE. THE FIGURE SHOWS A SERIES OF ASTER STEREO SCENES, WITH REGIONS OF OVERLAP DEPICTED BY THE DASHED LINES; THE DISTRIBUTION OF GCPs IS DEPICTED BY DOTS. STEREO PAIR "A" SATISFIES THE FOUR GCPs/SCENE REQUIREMENT. STEREO PAIR "B" HAS NO GROUND CONTROL POINTS, BUT AN ABSOLUTE DEM CAN BE GENERATED FOR THIS SCENE BECAUSE CONTINUOUS CONTROL IS AVAILABLE ALONG ITS UPPER AND LOWER EDGE FROM ABSOLUTE DEMs GENERATED FROM ADJACENT SCENES WITH GROUND CONTROL. A SIMILAR CASE EXISTS WITH SCENE "D". SCENES LABELLED "E" ARE WITHIN A BOX REPRESENTING THE AREA COVERED BY A UTM-PROJECTED TM SCENE OR BY A 1:50,000 SCALE TOPOGRAPHIC MAP. REGISTRATION OF THESE SCENES TO THE TM SCENE OR TOPOGRAPHIC MAP AND USE OF AS FEW AS TWO GCPs SHOULD BE SUFFICIENT TO MEET THE PLANIMETRIC ACCURACY SPECIFICATIONS.

option. This requires one dedicated work station with commercially available software and two operators.

3.2.2 Calibration and Validation

An overview of ASTER data product calibration and validation (including standard product DEMs) is provided in Thome et al. (1998). Planimetric and heighting calibration of ASTER DEMs is provided by GCPs. In situations where one or fewer GCPs are used, planimetric calibration will be inherited from the input Level 1, band 3N data product (Figure 1.0-1). This calibration information is documented in the algorithm theoretical basis document for the ASTER Level 1 data product, which is summarized in Fujisada (1998).

Because of the well established and operational nature of the DEM generation algorithm (Ackermann, 1994, and Figure 2.0-3), its validation is unnecessary. We will, however, specify performance standards and test the PCI system (Figure 3.0-1).

Figure 3.1-1 provides an example of one of the three methods that will be used to validate the accuracy of ASTER DEMs. Over the 11 validation sites that were selected by the ASTER Science Team (Table 3.2-1), we plan to subtract Z values from highly accurate DEMs, obtained from other sources, from Z values from ASTER DEMs covering the same sites, on a pixel-by-pixel basis. Results will be reported in the same format as Figure 3.1-1 and RMSEz values will be calculated under the assumption that the highly accurate DEM values are correct. Minimum, maximum, means and 1 sigma difference values will also be determined. In order to validate the planimetric accuracy of ASTER DEMs, we will use two other methods to validate ASTER DEMs for the 11 validation sites: 1) measure X-Y displacement of distinct topographic features on elevation profiles derived from ASTER DEMs with respect to the same features on the same lines of profile derived from 1:25,000 scale or better topographic maps or DEMs from other sources (a method discussed by Giles and Franklin, 1996); and 2) measure X-Y displacements of GCPs that were not used for DEM production (a method discussed by McGwire, 1996). Repeat measurements of these three validation parameters for the 11 validation sites, at least once per year using DEMs from newly acquired ASTER stereo pairs, will validate system stability over the six year mission. All of these validation data will be archived at the Land DAAC.

3.2.3 Quality: Assessment, Control and Diagnostics

The relevant quality control and related metadata information that will be provided in the header of each ASTER DEM are identified on Table 3.2-2.

3.2.4 Exceptional Handling

As part of our definition of the specific objective of the ASTER along-track stereo experiment (Section 2.1) we are identifying regions where stereo correlations will probably be poor. These areas will probably produce poor DEMs and/or require more operator intervention than elsewhere.

TABLE 3.2-1. ASTER DEM STANDARD PRODUCT VALIDATION SITES (LISTED IN PRIORITY ORDER).

SITE	PI
Mt. Kiso-Komagatake, Japan	Arai, Saga University
Huntsville, Alabama	Welch, University of Georgia
Mt. Fuji, Japan	Murakami, Geographical Survey Institute, Japan
Taxco/Iguala, Mexico	Lang, JPL
Mt. Tsukuba, Japan	Murakami, Geological Survey Institute, Japan
Drum Mountains, Utah	Bailey, USGS-EDC
Mt. Aso, Japan	Miyazaki, Geological Survey of Japan
Mt. Etna, Italy	Pieri, JPL
Mt. Unzen, Japan	Murakami, Geographical Survey Institute, Japan
Saga Plain, Japan	Arai, Saga University
Lake Okoboji, Iowa	Bailey, USGS-EDC

An important recommendation of the ADEMWG (Appendix 6-1) that would be exceptional handling, based on the present concept of allowable EOS data formats, is that ASTER Band 3N and 3B, SOM-projected Level 1B image data products be available in 1:250,000 scale, photographic hardcopy format. We believe that there will be substantial demand by the science user community for pictures of this type for stereoscopic viewing, manual interpretation and analysis. But although past experience (e.g., Berger et al., 1992, and Nishidai, 1993) with data from all high resolution, orbital, land imaging systems support this expectation, no plan exists for producing any EOS data in hard copy format at the DAAC.

4.0 Constraints, Limitations, Assumptions

All constraints, limitations and assumptions used to prepare this document are described elsewhere in the document, and therefore are not repeated here.

TABLE 3.2-2. RELEVANT QUALITY ASSURANCE AND RELATED METADATA REPORTED IN HEADER RECORD FOR EVERY STANDARD PRODUCT ASTER DEM.

1. CARRY THROUGH FOR THE TWO LEVEL 1 INPUT SCENES (3N AND 3B)
   a. Scene dates
   b. Scene-unique ID numbers
   c. Cloud assessment — percent
   d. Bad/suspect pixel QA image data plane

2. GCP INPUT DATA
   a. Number
   b. Locations — line and sample
   c. Locations — x, y, z and horizontal and vertical reference datums
   d. Provider(s) — name and address, etc.
   e. Source — e.g., GPS instruments type, surveying, map, photogrammetry
   f. Type of feature - e.g., road intersection, stream intersection

3. PRODUCT SPECIFICATIONS
   a. Cell spacing
   b. Relative or absolute
   c. % successful correlations
   d. Correlation method and matrix/window size used
   e. Lowest and highest elevation values
   f. Filtered or not — type filter used
   g. Edited — yes or no
   h. Overall quality assessment per operator and TBD criteria (1, 2 or 3)
   i. Correlation coefficient QA image data plane

5.0 Bibliography

Ackermann, F., 1984, Digital image correlation: performance and potential application in photogrammetry: Photogrammetric Record, v. 11, n. 64, p. 429-439.

Ackermann, F., 1994, Digital elevation models — techniques and application, quality standards, development: International Archives of Photogrammetry and Remote Sensing, v. 30, p. 4, p. 421-432.

Al-Rousan, N., P. Cheng, G. Petrie, T. Toutin, and M.J. Valadan Zoej, 1997, Automated DEM extraction and orthoimage generation from SPOT Level 1B imagery: Photogrammetric Engineering and Remote Sensing, v. 63, n. 8, p. 965-974.

Al-Rousan, N., and G. Petrie, 1998, System calibration, geometric accuracy testing and validation of DEM and orthoimage data extracted from SPOT stereopairs using commercially available image processing systems: International Archives of Photogrammetry and Remote sensing, v. 32, part 4, p. 8-15.

Al-Rousan, N., G. Petrie, T.R. Jordan, R. Welch, and H. Lang, 1998, Geometric accuracy of DEMs and orthoimages extracted from SPOT stereopairs using a low cost PC-based softcopy system: Technical Papers, ASPRS-ARTI 1998 Annual Conference, Tampa, Florida, March 30-April 3, p. 1230-1231.

American Society of Photogrammetry, 1952, Manual of Photogrammetry, 2nd ed.: Washington, DC, 876 p.

American Society for Photogrammetry and Remote Sensing, 1990, ASPRS accuracy standards for large-scale maps: Photogrammetric Engineering and Remote Sensing, v. LVI, n. 7, pp. 1068-1070.

Arai, K., 1992, Accuracy assessment of DEM with EOS-a/ASTER: Department of Information Science, Saga University, Japan, unpublished report to the ASTER DEM Working Group, 9 p.

Berger, Z., T. H. L. Williams, and D. W. Anderson, 1992, Geologic stereo mapping for geologic structures with SPOT satellite data: American Association of Petroleum Geologists Bulletin, v. 76, n. 1, p. 101-120.

Bohme, R., Compiler, 1993, Inventory of world topographic mapping: Elsevier, Permagon Press Inc., New York, The ICA International Cartographic Association, v. 1, 2 and 3, 1070 p.

Bolstad, P.V., and T. Stowe, 1994, An evaluation of DEM accuracy: Elevation, slope, and aspect: Photogrammetric Engineering and Remote Sensing, v. 60, n. 1, p. 1327-1332.

Borgeson, W. T., R. M. Batson, and H. H. Kieffer, 1985, Geometric accuracy of Landsat-4 and Landsat-5 Thematic Mapper images: Photogrammetric Engineering and Remote Sensing, v. 51, n. 12, p. 1893-1898.

Bureau of the Budget, 1947, United States National Map Accuracy Standards: U.S. Bureau of the Budget, Washington, DC, 1 p.

Cheng, P., and T. Toutin, 1998, Unlocking the potential for IRS-1C data: EOM, v. 7, n. 3, p. 24-26.

Clavet, D., M. Lasserre and J. Pouliot, 1993, GPS control for 1: 50,000-scale topographic mapping from satellite images: Photogrammetric Engineering and Remote Sensing, v. 59, n. 1, p. 107-111.

Derenyi, E., and L. Newton, 1987, Control extension utilizing Large Format Camera photography: Photogrammetric Engineering and Remote Sensing, v. 53, n. 5, p. 495-499.

Dowman, I., and F. Neto, 1994, The accuracy of along track sterescopic data for mapping: Results from simulations and JERS OPS: International Archives of Photogrammetry and Remote Sensing, v. 30, n. 4, p. 216-221.

DWG (DEM Working Group, Japan), 1997, ASTER DEM data product specification (Science Version), Version 2.1: Japan, ERSDAC Document, 79 p.

Ehlers, M., and R. Welch, 1987, Stereo correlation of Landsat TM images: Photogrammetric Engineering and Remote Sensing, v. 53, n. 9, p. 1231-1237.

Elassal, A.A., and V.M. Caruso, 1983, USGS digital cartographic data standards. Digital elevation models: U. S. Geological Survey, Circular 895-B, 40 p.

Fujisada, H., 1998, ASTER Level 1 data processing algorithm: IEEE Transactions on Geoscience and Remote Sensing, v. 36, n. 4, p. 1101-1112.

Fukue, K., H. Fujisada, and M. Tokunaga, 1996, New approach to ASTER orthoimage generation: Proceedings of the International Society for Optical Engineering, Infrared Spaceborne Remote Sensing IV, p. 98-105.

Gagnon, P.A., J.P. Agnard, C. Nolette, C., and M. Boulianne, 1990, A microcomputer-based general photogrammetric system: Photogrammetric Engineering and Remote Sensing, v. 56, n. 5, p. 623-625.

Gens, R., and J.L. Van Genderen, 1996, Review article SAR interferometry — issues, techniques, applications: International Journal of Remote Sensing, v. 17, n. 10, p. 1803-1835.

Gesch, D., 1993, Topographic data requirements for EOS global change research (4/30/93 draft): U.S. Geological Survey, EDC, Unpublished internal report for the LPDAAC Science Advisory Panel (in review), 57 p.

Giles, P.T., and S.E. Franklin, 1996, Comparison of derivative topographic surfaces of a DEM generated from stereoscopic SPOT images with field measurements: Photogrammetric Engineering and Remote Sensing, v. 62, n. 10, p. 1165-1171.

Gittings, B., 1993, Catalogue of digital elevation data (October, 1993): University of Edinburgh, unpublished listing with disclaimer, 8 p. [Available electronically at http://www.geo.ed.ac.uk/home/ded.html]

GSI, 1993, Report on the development of terrain relief measurement methods using JERS-1 stereo image correlation (in Japanese). Geographical Survey Institute (GSI) of Japan, 52 p.

Hohle, J., 1996, Experience with the production of digital orthophotos: Photogrammetric Engineering and Remote Sensing, v. 62, n. 10, p. 1189-1194.

Itek Optical Systems, 1981, Conceptual design of an automated mapping satellite system (MAPSAT): Itek Optical Systems, a Division of Itek Corporation, Lexington, Massachusetts, 285 p.

Kahle, A.B., F.D. Palluconi, S.J. Hook, V.J. Realmuto, and G. Bothwell, 1991, The Advanced Spaceborne Thermal Emission and Reflectance Radiometer (ASTER): International Journal of Imaging Systems and Technology, v. 3, p. 144 -156.

Kardoulas, N.G., A.C. Bird, and A.I. Lawman, 1996, Geometric correction of SPOT and Landsat imagery: A comparison of map- and GPS-derived control points: Photogrammetric Engineering and Remote Sensing, v. 52, n. 10, p. 1173-1177.

Kok, A.L., J.A.R. Blais, and R.M. Rangayyan, 1987, Filtering of digitally correlated Gestalt elevation data: Photogrammetric Engineering and Remote Sensing, v. 53, n. 5, p. 535-538.

Konecny, G., 1996, Paradigm changes in ISPRS from the first to the eighteenth congress in Vienna: Photogrammetric Engineering and Remote Sensing, v. 62, n. 10, p. 1117-1124.

Labovitz, M.L., and J.W. Marvin, 1986, Precision in geodetic correction of TM data as a function of the number, spatial distribution, and success in matching control points: a simulation: Remote Sensing of Environment, v. 20, p. 237-252.

Lang, H.R., and E.D. Paylor, 1994, Spectral stratigraphy: remote sensing lithostratigraphic procedures for basin analysis, central Wyoming examples: Journal of Nonrenewable Resources, Oxford Press, v. 3, n. 1, p. 25-45.

Lee, J.E. and S.D. Johnson, 1985, Expectancy of cloudless photographic days in the contiguous United States: Photogrammetric Engineering and Remote Sensing, v. 51, n. 12, p. 1883-1891.

Level-1 Data Working Group, 1995, Algorithm Theoretical Basis Document for ASTER Level-1 Data Processing: ERSDAC document LEL/7-13, version 2.1 (December 26, 1995), available from JPL ASTER Project Office, 107 p.

Li, R., 1998, Potential of high-resolution satellite imagery for national mapping products: Photogrammetric Engineering and Remote Sensing, v. 64, n. 12, p. 1165-1169.

Light, D.L., 1990, Characteristics of remote sensors for mapping and Earth science applications: Photogrammetric Engineering and Remote Sensing, v. 56, n. 12, p. 1613-1623.

Maruyama, H., R. Kojiroi, T. Ohtsuka, Y. Shimoyama, S. Hara, and H. Masaharu, 1994, Three dimensional measurement by JERS-1, OPS stereo data: International Archives of Photogrammetry and Remote Sensing, v. 30, p. 4, p. 210-215.

McGuire, K.C., 1996, Cross-validated assessment of geometric accuracy: Photogrammetric Engineering and Remote Sensing, v. 62, n. 10, p. 1179-1182.

Murphy, R.E., 1968, Map supplement no. 9 based on Goode base map: in, J.P. Tremblay, Cartography, New York, John Wiley and Sons.

National Aeronautics and Space Administration, 1979, Preliminary Stereosat mission description: Jet Propulsion Laboratory, California Institute of Technology, Pasadena, California, Publication 720-33, p. 1-1—12-9.

Nishidai, T., 1993, Early results from "Fuyo-1" Japan's Earth resources satellite (JERS-1): International Journal of Remote Sensing, v. 14, n. 9, p. 1825-1833.

Novak, K., and R. Tudhope, Editors, 1993, Foreword: Photogrammetric Engineering and Remote Sensing, v. 59, n. 11, p. 1609.

O'Neill, M.A., and I.J. Dowman, 1993, A simulation study of the ASTER sensor using a versatile general purpose rigid sensor modelling system: International Journal of Remote Sensing, v. 14, n. 3, p. 565-585.

Panton, D.J., 1978, A flexible approach to digital stereo mapping: Photogrammetric Engineering and Remote Sensing: v. 44, n. 12, p. 1499-1512.

Pearson, II, F., 1977, Map projection equations: Defense Mapping Agency, Washington, DC, Final Report TR 3624, 342 p.

Rao, T.C.M., K.V. Rao, A.R. Kumar, D.P. Rao, and B.L. Deckshatula, 1996, Digital terrain model (DTM) from India Remote Sensing (IRS) satellite data from the overlap area of two adjacent paths using digital photogrammetric techniques: Photogrammetric Engineering and Remote Sensing, v. 62, n. 6, p. 727-731.

Research and Engineering Directorate, 1984, LFC Payload: Lyndon B. Johnson Space Center, Houston, Publication JSC-18986, 1 sheet.

Scherrer, R., 1985, The WM GPS Primer: Satellite Survey Company, Wild-Heerbrugg Switzerland, 41 p.

Snyder, J.P., 1982, Map projections used by the U.S. Geological Survey: U.S. Geological Survey Bull., v. 1532, 313 p.

SPOT Image Corporation, 1993 (June), General information (DTM) SPOT digital terrain models: Reston, Virginia, SPOT Image Corp., 1 p.

Theodossiou, E.I., and I.J. Dowman, 1990, Heighting accuracy of SPOT: Photogrammetric Engineering and Remote Sensing, v. 56, n. 12, p. 1643-1649.

Thome, K., K. Arai, S. Hook, H. Kieffer, H. Lang, T. Matsunaga, A. Ono, F. Palluconi, H. Sakuma, P. Slater, T. Takashima, H. Tonooka, S. Tsuchida, R.M. Welch, and E. Zalewski, 1998, ASTER preflight and inflight calibration and the validation of Level 2 products: IEEE Transactions on Geoscience and Remote Sensing, v. 36, n. 4, p. 1161-1172.

Thorpe, J., 1996, Aerial photography and satellite imagery: Competing or complementary?: Earth Observation Magazine, v. 5, n. 6, p. 35-39.

Tokunaga, M., and S. Hara, 1996, DEM accuracy derived from ASTER data: Proceedings of the 17th Asian Conference on Remote Sensing, p. J-7-1 — J-7-5.

Tokunaga, M., S. Hara, Y. Miyazaki, and M. Kaku, 1996, Overview of DEM product generated by using ASTER data: International Archives of Photogrammetry and Remote sensing, v. 31, part B4, p. 874-878.

Topographic Science Working Group, 1988, Topographic Science Working Group report to the Land Processes Branch, Earth Science and Applications Division, NASA Headquarters: Lunar and Planetary Institute, Houston, Texas, 64 p.

Trinder, J.C., A. Vuillemin, B .E. Donnelly, and V.K. Shottigara, 1994, A study of procedures and tests on DEM software for SPOT images: International Archives of Photogrammetry and Remote Sensing, v. 30, p. 4, p. 449-456.

Tsu, H., Y. Yamaguchi, and A.B. Kahle, 1996, ASTER science mission overview: Proceedings, The International Society for Optical Engineering, SPIE v. 2817, p. 52-59.

University NAVSTAR Consortium, 1993, UNAVCO News: UNAVCO, P.O. Box 3000, Boulder, CO 80307, Summer 1993 Issue, 4 p.

von Grüber, O., 1930, Photogrammetry. Collected essays and lectures. English Translation: Amer. Photogr. Publ. Co., Boston, 1932 p.

Welch, R., 1980, Measurements from linear array camera images: Photogrammetric Engineering and Remote Sensing, v. 46, n. 3, p. 315-318.

Welch, R., 1989, Desktop mapping with personal computers: Photogrammetric Engineering and Remote Sensing, v. 55, n. 11, p. 1651-1662.

Welch, R. and W. Marko, 1981, Cartographic potential of spacecraft line-array camera system: Stereosat: Photogrammetric Engineering and Remote Sensing, v. 47, n. 8, p. 1173-1185.

Welch, R., and D. Papacharalampos, 1992, Three-dimensional terrain visualization on personal computers: an application with stereo SIR-B images: Photogrammetric Engineering and Remote Sensing, v. 58, n. 1, p. 71-75.

Welch, R., T.R. Jordan, and M. Ehlers, 1985, Comparative evaluations of the geodetic accuracy and cartographic potential of Landsat-4 and Landsat-5 Thematic Mapper image data: Photogrammetric Engineering and Remote Sensing, v. 51, n. 9, p. 1249-1262.

Welch, R., T.R. Jordan, and J.C. Luvall, 1990, Geocoding and stereo display of tropical forest multisensor datasets: Photogrammetric Engineering and Remote Sensing, v. 56, n. 10, p. 1389-1392.

Welch, R., T. Jordan. H. Lang, and H. Murakami, 1998, ASTER as a source for topographic data in the late 1990's: IEEE Transactions on Geoscience and Remote Sensing, v. 36, n. 4, p. 1282-1289.

Willard, J. H., 1992, Data base blending for the climatology of cloud statistics program: Phillips Laboratory, Hanscom Air Force Base, Massachusetts, Publication PL-TR-92-2344, 57 p.

Wolf, M., and D. Wingham, 1992, The status of the world's public-domain digital topography of the land and ice: Geophysical Research Letters, v. 19, n. 23, p. 2325-2328.

Yamaguchi, Y., H. Tsu, and H. Fujisada, 1993, A scientific basis of ASTER instrument design: SPIE Proceedings, p. 150-160.

Yamaguchi, Y., A.B. Kahle, H. Tsu, T. Kawakami, and M. Pniel, 1998, Overview of Advanced Spaceborne Thermal Emission and Reflection Radiometer (ASTER): IEEE Transactions on Geoscience and Remote Sensing, v. 36, n. 4, p. 1062-1071.

APPENDIX 6-1

MEMBERSHIP AND CHARTER OF THE ASTER DIGITAL ELEVATION MODEL WORKING GROUP (ADEMWG) (8/16/96)

MEMBERS

CO-CHAIR. Y. Miyazaki, Geological Survey of Japan, H. Murakami (Acting), Geographical Survey Institute of Japan; and Roy Welch, University of Georgia.

MEMBERS. M. Abrams, JPL; K. Arai, Saga University; B. Bailey, USGS; H. Lang, JPL; H. Maruyama, Geographical Survey Institute of Japan; S. Obayashi, Science University of Tokyo; T. Osanai, JAPEX Geoscience Institute; D. Pieri, JPL.

CHARTER

The purpose of the ASTER Digital Elevation Model Working Group (ADEMWG) is to provide:

a. Overall direction for the creation and validation of ASTER digital topographic models based on the ASTER stereo viewing capability.
b. A forum to explore and evaluate innovative techniques and applications for ASTER stereo data.

The ADEMWG will review the Level 1 Data Working Group's software implementation activities in order to confirm that appropriate software routines are in place prior to the EOS-AM1 Platform launch.

Some aspects of this effort include:

1. Developing ASTER simulation test data sets for prelaunch algorithm studies.
2. Understanding platform stability, position knowledge, and jitter issues with regard to DEM precision and accuracy, and providing science requirement inputs to the EOS Project in that context.
3. Consulting with the ASTER instrument design team on DEM science requirements.
4. Defining the ASTER DEM data product format.
5. With the ASTER Level 1 (Geometry) Working Group, developing specifications for the content and format of a Ground Control Point (GCP) library and recommending a process for building ("populating") the GCP library.
6. With the Level 1 Working Group, recommending the coordinate system and resolution to be used for Level 1 data products.

APPENDIX 6-2

AUTOMATIC STEREO CORRELATION ALGORITHM FOR GENERATING DEMs FROM DIGITAL STEREO DATA THAT WAS CONSIDERED FOR THE STEREOSAT MISSION (EXTRACTED FROM NATIONAL AERONAUTICS AND SPACE ADMINISTRATION, 1979). THIS EXAMPLE IS PROVIDED AS AN ILLUSTRATION ONLY. THE ACTUAL ALGORITHM THAT WILL BE USED FOR ASTER AUTOMATIC STEREO CORRELATION WILL PROBABLY BE PROPRIETARY, IN DETAIL BECAUSE WE WILL USE OFF-THE-SHELF COMMERCIAL SOFTWARE.

9.4 DIGITALPHOTOGRAMMETRY

Because Stereosat images are already in digital format, and because geometric deviations between adjacent images are expected to be less than a single pixel, it is an attractive idea to try to produce DEMs directly by digital cross-correlation. Similar efforts have been successful in part although somewhat expensive, so this technique may not be appropriate for mass production, but just for regions which are exceptionally interesting. Plans and preliminary results for such a procedure are outlined below.

9.4.1 Method

The method actually used to compute DEMs from convergent line-array stereo pairs is rather straightforward, but time-consuming. Essentially, a cross-correlation must be performed between one of the pictures, called the reference image, and the other, here called the displaced picture. Because only the component of parallax which is parallel to the base-line (along-track) differs between the two pictures, in the ideal case a one-dimensional cross-correlation is adequate to compute parallax. In the real case we must expect residual geometric errors of about one pixel in the cross-track or scan direction caused by spacecraft attitude changes between pictures. Because of this, the cross-correlation window should probably measure three pixels in the scan direction rather than one. The actual cross-correlation algorithm for discrete images is given by

$$c(s, t, p) = \sum_{i=-1}^{1} \sum_{j=-N}^{N} REF(s+i, t+j)\, DISP(s+i, t+j+p) \qquad (9\text{-}4)$$

where s and t are the pixel coordinates of the spot being evaluated in the scan and track directions, p is the parallax, 2N + 1 is the dimension of the correlation window in the track direction, c is the cross-correlation coefficient, and REF and DISP are brightness values or gray levels from the reference and displaced images. This expression must be evaluated for all points in the reference image (s, t) and for all

parallaxes possible at each point. Because parallaxes are not generally integer values, this latter requirement cannot be met. Instead, c for a sampling of possible parallax values is evaluated, and the exact parallax is estimated by interpolating a polynomial least squares fit to the c values to find the maximum cross-correlation, which coincides with the best registration of the two images at the point (s, t) being considered.

In practice, values of C may be normalized by the auto correlation of the reference image, so that

$$c(s, t, p) = \frac{\sum_{i=-1}^{1} \sum_{j=-N}^{N} REF(s + i, t + j)\, DISP(s + i, t + j + p)}{\sum_{i=-1}^{1} \sum_{j=-N}^{N} REF(s + i, t + j)^2} \qquad (9\text{-}5)$$

This has the effect of removing regional brightness gradients from c, making interpretation of the performance of the algorithm simpler. Finally, it has proven desirable in the past to further remove the effects of brightness gradients and, in fact, brightness differences between equivalent points in the reference and displace images, using a high-pass filter. Brightness differences can easily develop in different pictures of the same scene because of changes in the viewing angle. This is not true for a Lambert surface because the decrease in radiative flux with oblique viewing angles is exactly compensated by the increased area of the IFOV; but, for different real surfaces (e.g., a specular surface) brightness differences can be significant. The high-pass filter, which exaggerates edges and small detail and suppresses regional brightness variations, must be carefully chosen to minimize ringing and the introduction of directional artifacts, as well as to avoid undue exaggeration of high-frequency noise. Thus if a uniform-weight or "box" filter is used, the cross-correlation algorithm as implement is given by

$$c(s,t,p) = \frac{\sum_{i=-1}^{1} \sum_{j=-N}^{N} \left[REF_{(s+i,\, t+j)} - (2m+1)^{-1}(2n+1)^{-1} \sum_{k=-m}^{m} \sum_{j=-n}^{n} REF_{(s+i+k,\, t+j+l)} \right] \left[DISP_{(s+l,\, t+j+p)} - (2m+1)^{-1}(2n+1)^{-1} \sum_{k=-m}^{m} \sum_{i=-n}^{n} DISP_{(s+i+k,\, t+j+p+i)} \right]}{\sum_{l=-1}^{1} \sum_{j=-N}^{N} \left[REF_{(s+i,\, t+j)} - (2m+1)^{-1}(2n+1)^{-1} \sum_{k=-m}^{m} \sum_{l=-n}^{n} REF_{(s+i+k,\, t+j+p+i)} \right]}$$

In practice, cross-correlation is performed on pictures which have been filtered already. In this way, computational short-cuts in the filtering may be utilized, which reduces running time.

Choice of the window sizes used in filtering (m and n) and in cross-correlation (N) may be left to the analyst and may, in fact, be varied from scene to scene. Choice

of the order of the polynomial used to fit the array of correlation coefficients at each pixel (for different values of parallax) is also open, as is the number of c values used to specify the polynomial. Computational costs increase with the number of points used, while, if the order is too high, stability of the solution is reduced (there may be spurious peaks in the polynomial). If the order is too low, resolution in the estimation of the actual parallax may be lost.

If, instead of interpolating to find the actual parallax, the nearest integer value of parallax is adopted, then for a stereo pair consisting of a down-looking and an oblique line-array image, the elevation may be measured only to the nearest 15 meters. On the other hand, by interpolating the parallax it should be possible to identify the best registration to within perhaps 0.25 pixels, leading to an elevation resolution of four meters.

It should be emphasized that the accuracy of this method is predicated on accurate knowledge of spacecraft altitude and attitude. Consequently, while relative topography maybe readily derived, DEMs of cartographic quality will probably require fitting to several ground control points.

APPENDIX 6-3
WHITE PAPER ON DEM PRODUCTION OPTIONS (9/27/94)

Options for the Production of DEMs as Standard ASTER Data Products

by
EOS ASTER Science Team Topographic Working Group
and
Land Processes DAAC Topographic Data Team

1.0 Introduction

1.1 Purpose

The purpose of this paper is to endorse digital elevation models (DEMs), produced from ASTER stereo data at the Land Processes DAAC, as a standard EOS data product. Furthermore, this paper presents the characteristics and estimated costs of three alternative production capabilities ranging from 1 DEM per day to 25 DEMs per day.

1.2 Scope

This paper summarizes requirements for an ASTER DEM standard product and describes the components and characteristics of a representative DEM production system. Capability and cost options for an actual DAAC system also are provided. A basic assumption of this analysis is that the system and capabilities endorsed here are intended to meet specific data processing and science requirements of individual users, and they are not intended to be a "global DEM production system". However, it should be recognized that ASTER-based DEMs produced at the Land Processes DAAC would be archived there, along with qualifying DEMs produced elsewhere, leading to a gradual buildup of a library of DEMs for areas from around the world. This paper is intended only as a contribution to the decision-making and planning processing. Any necessary implementation documents will be written once a specific option is selected.

1.3 Background and Status

The general configuration of the Earth's land surface, including its relief and the position of its natural features, is the physical earth property commonly referred to as "topography". In spite of being perhaps the most fundamental and evident of Earth's geophysical properties, the detail and accuracy with which the Earth's topography has been measured and des-

cribed, particularly on a global scale, is surprisingly poor. For example, the highest resolution topographic data, with global coverage and public availability in digital form, are the ETOP05 data which have elevations posted every 10 kilometers.

Literally all disciplines of scientific study involving the Earth's land surface exploit topographic data and/or their derivative measurements of slope and aspect. In recent years, with growing public awareness of environmental issues and increasing emphasis on global change science, requirements for digital topographic data have both increased and become more rigorous. Certainly, this is the case as pertains to EOS, where new and variably strict requirements have scientists, engineers, and program managers alike scrambling to identify existing and/or new DEMs with sufficient resolution and accuracy to meet their requirements.

Between now and the launch of EOS-AM1, the likelihood is good that there will be at least an order of magnitude improvement (to 1 km) in the resolution of the best available **global** DEM. Assuming public release of the Defense Mapping Agency's digital terrain elevation data (DTED), up to 75% of the Earth's land surface will have DEM coverage available with 100-meter grid spacing and vertical accuracy of 30 meters. Nevertheless, many important EOS-related DEM data requirements will remain unsatisfied (Topographic Science Working Group, 1988). However, the opportunity exists to meet certain of the more rigorous requirements by producing, on a routine basis, some quantity of DEMs derived from stereo image data acquired by ASTER.

2.0 Product Description

2.1 Definition

The ASTER DEM standard product will be a regular grid of elevation values recorded in units of whole meters. The cell dimension (posting) will be either 30 meters or 60 meters as described in the ASTER DEM ATBD. The DEM, covering an area equal to the nadir image of 60 x 60 kilometers, will be referenced in the UTM projection coordinate system. DEMs normally will not be produced unless virtually cloud-free stereo data have been acquired.

2.2 Accuracy and Scale

Accuracy of the absolute DEM product will be measured by calculation of the root mean square error (RMSE). The ASTER DEM Working Group has conducted several studies that show the expected vertical RMSE is in the 7-50 meter range. The number and accuracy of the control points used for

rectification of the stereo pair have a significant effect on the resultant DEM accuracy. The test results also show that a slope accuracy of 5 degrees should be attainable from ASTER DEMs when slopes are determined over a measurement distance greater than 100 meters. The DEM Working Group has estimated conservatively that ASTER DEMs will be useful for mapping in the 1:100,000- to 1:250,000-scale range, and in some cases even for 1:50,000-scale applications (Lang and Welch, 1994).

2.3 Relative or Absolute

The ASTER DEM will be absolute (in reference to mean sea level) when suitable ground control points (with known X, Y, X) are available for rectification of the stereo pair. Topographic map sources ranging from 1:25,000- to 1:100,000-scale should provide control of sufficient accuracy for processing ASTER stereo data. When ground control is not available, a relative DEM still may be produced.

3.0 Rationale and Justification

3.1 General Requirements

Topographic data requirements for EOS can be divided into two general categories: instrument and science. Instrument requirements are those related to the processing of the sensor data to produce a set of radiometrically and geometrically corrected data products. DEM resolution and accuracy requirements vary and depend primarily on the resolution of the sensor data being corrected. ASTER, MODIS, MISR, and CERES on the AM1 Platform have instrument-related topographic data requirements, as do AIRS and EOSP (see Gesch, 1994).

Science requirements are those that relate to the ability of the user to develop and generate higher-order data products which present specific geophysical variables or affect the user's ability to interpret scientific information or model physical processes. knowledge of slope needed in calculating basin run-off or in modeling the advance of a glacier and knowledge of elevation and aspect needed to model rate of snow melt are but a few examples of the many and varied science requirements that will be levied on topographic data during the EOS time frame. Here again, DEM resolution and accuracy requirements vary depending on research objectives and on sensor resolution. However, in general, science requirements levied on topographic data are more rigorous than instrument requirements because of the scale on which many processes of interest operate. Consequently, the significance of ASTER as a potential source of DEM data for certain process-based and site-specific studies must be recognized.

3.2 Specific Requirements

In-depth analyses of general and specific topographic data requirements for EOS specifically, and earth science studies in general are presented by Gesch (1994) and the NASA Topographic Science Working Group (1988), respectively. Such in-depth treatment of requirements is beyond the scope of this paper, suffice to say that the ASTER DEM has significant potential for meeting certain identified EOS instrument and science topographic data requirements, some of which are noted below.

Most MODIS and MISR topographic data requirements related to radiometric and geometric correction can be met by a DEM with 100 meter grid spacing and a vertical accuracy of 30 meters (Gesch, 1994). As noted above, a DEM that meets these criteria may be available for 75% of the Earth's land surface by EOS-AM1 launch. For the remainder of the Earth's land surface, another source of digital topographic data will be required. ASTER-derived DEMs may be the only alternative, for some parts of the world, with the potential to meet the grid spacing and vertical accuracy requirements. Topographic data requirements for radiometric and geometric correction of ASTER data have not yet been definitively established. However, it is clear that the precision and accuracy of such corrections will improve with higher resolution and more accurate DEMs. Consequently, availability of ASTER-derived DEMs for areas where DEMs with 15-meter (or better) grid spacing and 7-meter to 50-meter vertical accuracy do not exist will improve ASTER radiometric and geometric correction capabilities. Furthermore, it is important to recognize that the precision, accuracy, and ultimate usability of all subsequent products, generated from radiometrically and/or geometrically corrected MODIS, MISR, or ASTER data are strongly influenced by the precision and accuracy of those initial corrections.

Specific examples of this latter point exist with respect to four or five of the other Level 2 ASTER standard data products. These products either generate atmospherically corrected radiances or use atmospherically corrected ASTER data as input to the product. Consequently, the precision and accuracy of those products will be greater in instances where the DEMs used to correct the data had finer resolution grid spacing and greater vertical accuracy.

Thirteen of 29 EOS IDS teams have identified topographic data specifically as an input data set required for them to generate science products or interpret information from EOS data. Of these, seven teams have indicated that some or all of their requirements can be met by ASTER DEMs. Examples of products or information required by IDS investigators include topographic elevation and slope, land surface roughness, ice sheet elevation, and volcano elevation. Clearly, selected production of ASTER

DEMs will contribute substantially to the ability of scientists to meaningfully analyze EOS data and to make interpretations necessary for understanding global change processes.

3.3 DAAC Location Rationale

Substantial and significant EOS requirements exist for ASTER-derived DEMs to be produced. Consequently, it is incumbent upon the EOSDIS project to provide that capability in support of EOS scientists, and it is only logical that such a capability be located at the Land Processes DAAC where other ASTER data products are produced. This is not to say, however, that ASTER DEMs should not be produced elsewhere by others qualified to do so. In fact, DEM generation by other science users and commercial entities should be encouraged as a mechanism to more rapidly expand coverage by higher-resolution DEMs. Pursuant to this goal, the LPDAAC should establish and encourage population of a central DEM repository, leading to the gradual buildup of a library of DEMs, and perhaps associated ground control, thereby eliminating the necessity to recompute DEMs for the same ground location. The institutional expertise resident at the DAAC would be applied not only to providing science support to users (and other producers) of ASTER DEMs, but also to setting standards and monitoring the quality of DEMs produced by others for inclusion in the central repository.

4.0 Product Generation System

4.1 General Description

The ASTER DEM product generation system (PGS) will be located at the LPDAAC. The assumption here, as stated in the ASTER DEM Algorithm Theoretical Basis Document (ATBD), is that the DEM PGS will be based on commercial-off-the-shelf (COTS) components. Generation of DEMs from digital stereo imagery is a well established technique, and as such, there is a good variety of fully functional systems offered commercially. A review of the 1994 ASPRS Directory of the Mapping Sciences shows that at least 15 vendors offer systems for DEM production.

ASTER Level 1 data will be the input for the ASTER DEM system. If ground control point processing is not part of the standard Level 1 processing (not currently planned), then the DEM system must have the capability for selection and use of ground control points. if the DEM system needs control point capabilities, additional peripheral input devices (e.g., digitizing table or map scanner) would be required. If the Level 1 ASTER stereo data are registered and geocoded before ingest to

the DEM system then the required functionality of the DEM software is simplified.

4.2 Key Elements and Options

4.2.1 Hardware

The available DEM packages run on a wide variety of hardware platforms, but the most common is the workstation class machine. Some systems are also available for personal computers. While the choice of hardware for the DEM PGS ultimately will be based on the required throughput capacity, it is envisioned that the package will reside on one or several workstations with network access to the necessary peripherals. Some DEM packages make use of special image processing boards in addition to the main CPU for the compute-intensive processing such as resampling and correlation. Requirements for any special processing hardware will be driven by the particular DEM production package selected.

An important hardware component for any DEM system is the stereo display. Stereo viewing of the source imagery is crucial for the operator during editing and validation stages of product generation. Graphics are superimposed in three dimensions to provide the operator with visualizations of the DEM over the stereo pair. Several techniques are employed to display stereo images on a computer monitor, including passive display with polarized glasses and monitor, active display with shuttered glasses synchronized to the monitor, and anaglyphic display on a standard color monitor viewed with anaglyphic glasses.

4.2.2 Software

The COTS DEM generation software must have a wide array of functionality. An important characteristic is that it must be able to handle various forms of ASTER stereo data, i.e., single 60 x 60 km scenes and longer swaths. The system should allow production of a relative DEM in the absence of suitable ground control, as described in the ASTER DEM ATBD. The system should be programmable to the greatest extent possible, allowing batch processing and stringing together the various stages of DEM production, thus reducing the requirement for operator intervention. Computational speed and efficiency of the software also are critical characteristics, but the requirements for such are driven by the throughput capacity ultimately specified for the DEM PGS.

It is envisioned that the most effective user interface will be one that is highly graphical and intuitive in nature. This is especially important for the labor intensive functions which require an operator to interact extensively with imagery and graphics, such as control point selection

and DEM editing and validation. Features of the software which will enhance productivity and output product quality include: a diverse suite of DEM editing and filtering tools; the ability to import and use ancillary topographic information, such as geomorphic feature data derived form other sources, in the correlation and editing processes; creation and easy access to a "measurement quality" data set registered to the DEM as an aid for editing and quality assurance; block adjustment of input imagery so that available ground control can be extended to simultaneously correct a block of adjacent scenes prior to correlation; expression of parallax translated into DEM vertical units during editing to increase the operator's intuitive feel for DEM quality; and selection of various correlation strategies to that DEM generation can be optimized for specific image and terrain conditions.

4.2.3 Operations

Operation of the DEM PGS will be integrated into the larger LPDAAC product generation capability. As currently projected, the DEM PGS will be of a smaller scale (one to several workstations) that can be run efficiently by only one or two operators per shift. Much of the DEM generation process, especially resampling and correlation, can run unattended, so the operator can perform the necessary interactive processing while just being available to monitor the background processing. Operators will be required to have the necessary photogrammetric training and knowledge to generate digital topographic data.

4.2.4 Quality Assurance

As outlined the ASTER DEM ATBD, validation will consist of quantitative comparison of ASTER DEMs with highly accurate DEMs from other sources over selected test sites. Much of this work could be accomplished at the LPDAAC with the DEM PGS itself. The PGS should have wide ranging capabilities for visualization of the DEM and, if corresponding highly accurate DEMs exist, statistical reporting capabilities to fully describe the accuracy and quality. Another useful quality assurance approach involves creating and plotting derivative products from the DEM (slope, aspect, shaded relief, perspective views, basins, ridges, flowlines, etc.) as many times these products show evidence of data anomalies not readily seen in other standard representations of the DEM. Another important aspect of quality assurance is the consistency of data in the overlap areas of adjacent DEMs, and this must be monitored routinely.

4.2.5 Maintenance

System maintenance is to be provided by the vendors. Particularly important are resolution of problem reports, enhancement requests, and upgrades for the DEM generation software. Open access to the system would facilitate implementation of improvements to correlation, editing tools, or filtering routines developed at the LPDAAC or by the ASTER Science Team.

4.3 Scalability Issues

Of utmost importance for the DEM PGS residing at the LPDAAC is that it be scalable. If demand for ASTER DEMs is great, the system may have to be augmented to increase its production capacity. The configuration must not be so rigid that the only way to increase capacity is to add complete, identical systems. A more economic and efficient approach would perhaps be to just add the necessary software modules and hardware components and to operate subsystems for specific tasks, e.g., control point selection, resampling and correlation, visual editing, and output.

5.0 Capability and Cost Scenarios

5.1 Background

Numerous variable affect the production and cost of digital elevation data generation. Data preprocessing, postprocessing, system functionality and capability, quantity and quality production requirements, and the skill of the system operator(s) are some of the factors that can significantly affect production rates and costs. In this section, estimates are presented of the resources required to implement and maintain a digital elevation model (DEM) production capability at three levels: one scene per day, 10 scenes per day, and 25 scenes per day. Work hour estimates are based on recent experience in generating DEMs from satellite data, and they assume that ground control point data which may be applied are readily available to the operators.

5.2 One Scene Per Day (365 scenes per year)

A production level of one scene per day would enable the Program to develop and maintain a high level of expertise, albeit limited to a small number of individuals, and to meet a number of EOS-related requirements for DEM data. Production of one scene per day could be accomplished with one dedicated workstation, host computer, software and peripheral devices, capable of performing image preprocessing, DEM generation and

postprocessing functions. It would require two operators performing interactive tasks, primarily pre- and postprocessing tasks, about 80 hours per week. (Six to eight hours of preprocessing, two to four hours of postprocessing, and one hour miscellaneous activities per scene.) Background or batch tasks (DEM generation) would likely be ongoing 24 hours per day.

Using current cost figures, acquisition of workstation with the required capability likely would cost in the neighborhood of $150K. Two full-time operators would be about $200K per year, and maintenance, supplies, and training about $25K per year. Based on the above estimates and a five year life time, the yearly cost of this scenario is about $260K, or somewhat more than $700 per scene.

5.3 Ten Scenes Per Day (3650 scenes per year)

This level of production would meet most, if not all, of the EOS-related requirements for DEM data. At this level of production, some economy of scale could be realized. Both personnel requirements and hardware/software costs per DEM could be substantially reduced. Hardware, software, and personnel would perform specific tasks within the processing flow rather than end-to-end processing, and data could be processed more efficiently; for example, processing swaths of imagery rather than single scenes.

Using current cost figures, the total expenditure for hardware and software would be in the neighborhood of $1 million. The system would require perhaps 15 to 17 full time personnel (about $1.7 million per year), and training, maintenance, and supplies would be about $100K per year. Based on the above estimates and a five year lifetime, the yearly cost of this scenario is about $2 million, or somewhat less than $550 per scene.

5.4 Twenty-five Scenes Per Day (9000 scenes per year)

At this level of production nearly every cloud free stereo pair of imagery acquired would be processed into a DEM. (ATBD for ASTER Digital Elevation Models, Section 2.0.) Again, some economy of scale could be realized, but at this level of production estimates of costs or savings associated with individual system components would be very uncertain without much more extensive study. However, an assumption that the cost per unit product could be reduced by a factor 10 percent relative to the cost per unit product at the 10-scene-per-day production level is not unreasonable.

Based on the above assumption and a five year life time, the yearly cost of this scenario is about $4.5 million, or about $500 per scene.

6.0 Summary and Conclusions

Still at issue in the development of EOSDIS in general, and capabilities at the Land Processes DAAC specifically, is the question of whether or not an ASTER-based DEM will be provided as an ASTER standard data product. Prompt resolution of this issue is needed.

Generation of a global DEM is well beyond the scope and feasibility of an ASTER standard product DEM generation capability. However, numerous important EOS instrument and science requirements exist, which are regional or site-specific in scope and which have the potential of being met by an ASTER DEM. These requirements justify the development and implementation of an ASTER DEM standard data product generation capability. Placement of such a production capability at the Land Processes DAAC is dictated by the logic of colocation with other ASTER standard product generation systems and ease of entry into a growing central repository of globally distributed DEMs.

At issue, then, is the size and scope of the ASTER DEM standard product generation system to be implemented. These should be determined based the best possible projection of user demand.

7.0 Selected References

Gesch, D.B., 1993, Identification of requirements and sources for global digital topographic data, in Pecora 12 Symposium, Land Information from Space-Based Systems, Sioux Falls, South Dakota, August 1993, Proceedings: Bethesda, Maryland, American Society for Photogrammetry and Remote Sensing, in press.

Gesch, D.B., 1994, Topographic data requirements for EOS global change research: U.S. Geological Survey Open-File Report 94-626.

Lang, H.R., and Welch, R., 1994, Algorithm Theoretical Basis Document for ASTER Digital Elevation Models: Jet Propulsion Laboratory, May 31, 1994, draft report to the EOS Project.

Muller, J.P., 1993, Topography requirements for MODIS: University College London, unpublished report.

Schier, M., ed., 1993, The science objectives of the Advanced Spaceborne Thermal Emission and Reflectance Radiometer (ASTER): Jet Propulsion Laboratory, Pasadena, CA, unpublished report.

Science Processing Support Office (SPSO), 1992, Earth Observing System output data products and input requirements - version 2.0 (3 volumes): NASA Goddard Space Flight Center, Greenbelt, MD.

Topographic Science Working Group, 1988, Topographic science working group report to the Land Processes Branch, Earth Science and Applications Division, NASA Headquarters: Lunar and Planetary Institute, Houston, TX, 64 pp.

Wolf, M., and Wingham, D.J., 1992, A survey of the world's digital elevation data — Mullard Space Science Laboratory Report 4010/05-91/002: Mullard Space Science Laboratory, Dorking, Surrey, United Kingdom, 87 pp.

APPENDIX 6-4

WHITE PAPER ON GCPs
(4/14/94, BY EDC PERSONNEL)

GROUND CONTROL POINT LIBRARIES FOR THE PRECISION CORRECTION OF REMOTE SENSING IMAGERY

by D. R. Steinwand, C. E. Wivell, and L. R. Oleson

I. Introduction: The need for ground truth information

Spaceborne remote sensing imagery can provide a consistent, accurate view of the Earth's surface in a timely and repeatable fashion. Users of these data often wish to combine these data with data from other sources in a consistent geometric base, usually a map projection. This requires precision geometric correction, including terrain corrections, of the satellite imagery, often to subpixel accuracy.

The geometric accuracy of the image is directly related to the accuracy of the geometry models and the ancillary information used in the correction process. The geometric characteristics of the sensor (instrument) are usually well known and can be modelled accurately. When combined with satellite position and attitude information, this usually yields imagery with very good internal (relative) accuracy The absolute pixel-to-ground accuracy however is directly related to the knowledge of the satellite's position and attitude at a given instant of time.

Future satellite remote sensing systems maybe able to achieve subpixel accuracy using information directly from the satellite. However, most systems do not provide satellite position and attitude information with sufficient accuracy to achieve subpixel registration accuracy. For example, Landsat 4, 5 Thematic Mapper (TM) imagery which has been systematically corrected (using no ground control) to a map projection with a pixel size of 28.5 meters has been shown to be internally very accurate, but absolute image-to-ground measurements are not (Thormodsgard and DeVries, 1983; Welch and Usery, 1984). AVHRR imagery can display image-to-ground accuracies of 5-8 km when systematically corrected to a map projection and 1 km pixels. In order to achieve subpixel image-to-ground accuracy, additional information is required. In these and in other cases, ground control points can be applied to refine the satellite's position and attitude information. A ground control point is simply the iden-

tification of a pixel in the image and it's corresponding geographic location (usually latitude, longitude, elevation). These locations are measured to fractional pixel locations.

II. What is a GCP library and how is it used?

A ground control point library (GCPLIB) is a collection of image subwindows (often referred to as image "chips") which contain features that are measurable on some reference base (i.e., a map in many cases) for initial, manual selection, but that are also spectrally relevant to the matching algorithm in use. Each of these chips have associated with them a latitude, longitude, and elevation of a point marked in the chip, as well as other information as to the chip's origin and usage statistics. Usual sizes for image chips are 32 by 32 pixels or 64 by 64 pixels, although other sizes may also be used. Figure 1 shows a sketched example of a Landsat control point chip and associated information.

In general, the application of ground control points from a GCPLIB is as follows:

1. Using the ephemeris and attitude information collected with the scene to be registered and a geometric model of the satellite and sensor (systematic model), the geographic extent of the imagery to be registered is calculated.
2. Image chips and their associated data that are located within the geographic extent of the image are extracted from the GCP library. In fully populated GCPLIBs, additional information (such as band number or season/date) may be used to limit the number of chips extracted from the library.
3. For each chip extracted from the GCPLIB, the approximate corresponding location in the raw image is calculated using the systematic model.
4. Before the typical matching algorithms can be applied the projection and scale of the two surfaces to be matched must be the same — these matching algorithms can find displacements due mainly to translational errors; differences due to rotation or scaling effects can cause poor performance. Therefore, either the image chip from the GCPLIB is mapped to the geometry of the corresponding image neighborhood in the uncorrected image or vise versa.
5. Most current systems match GCPLIB chips with the imagery using variants of cross-correlation. One of the more commonly used variants is the normalized cross-correlation which adjusts the correlation surface for brightness differences in the image or

chip (Wood and Sellman, 1987; Kiss and others, 1981). Other variants include various edge enhancement techniques or phase-only adjustments (Pearson and others, 1977).

6. After point matching, the resulting image offsets between locations predicted by the systematic model and actual GCPLIB locations are used to update the geometry model parameters (usually time, roll, pitch, yaw, altitude, and their rates). During this update process, outliers or blunders in the matching process can be identified by relating updated model parameters to known physical limits of those parameters. This assist in constraining the correction.

The geometric base of the GCPLIB should be given some consideration. Some GDPLIBs store chips in path-oriented, basically raw (not map projected) geometry, whereas other GCPLIBs store ships in a map projection. Storing chips in a map projected format enhances their utility because the geographic locations of all pixels in the chip are known, not just the point selected for control pointing purposes. Storing a chip in a map projection also aids in the geometric transformation into raw image space as described in step 4 above.

Various schools of thought exist as to the best features to select as ground control point chips (Hogan and others, 1980). Some prefer land/water interfaces due to the large contrast between the two; this large contrast often aids in the automated matching process. Others prefer roads or other manmade features. The "best" feature is one that performs nicely with the matching algorithm used and one that does not change with time. Changes in spectral signatures due to different seasons, changing water levels, tides, and human-induced changes (new/different roads, new water bodies, different crop types or consideration when determining the characteristics of the GCPLIB. Static libraries — those that are built and left to run with little or no maintenance — may degrade in performance as time goes on due to ground feature changes. Some level of library maintenance or updates should therefore be built into the design of a GCPLIB system.

III. The number of chips required for correction

The number of ground control points required to correct a satellite image is dependent on a number of factors, such as the method used to geometrically correct the imagery, the stability of the sensor and satellite system, the accuracy of the knowledge of the attitude and ephemeris data, the accuracy of the control information, and the amount of cloud cover.

The two methods most commonly used to precisely geometrically correct satellite imagery are the warping of a systematically corrected image using polynomials, and updating the ephemeris and attitude data used in the satellite/sensor model. The image warping method first produces a systematic product (no ground control used) and then uses low order polynomials to fit ground control information to the systematic product. This results in an image product which has been resampled twice, but can also lead to problems in identifying outliers in the ground control points. A simple polynomial fit does not relate the control points back to the physical characteristics of the sensor/satellite, and may thus result in a "correction" (warp) which is not characteristic of the sensor's geometry. This method requires at least one control point for each of the coefficients used in the polynomial and the control points must be distributed throughout the image. These constraints cause the number of control points required to warp an image to be in the 15 to 25 point range when low order polynomials are used. In the second method, the correction of the ephemeris and attitude assumes the errors in the imagery are caused by biases mainly in the ephemeris and attitude data. This method requires at least three control points to find correction values for the bias errors of roll, pitch, yaw and altitude and the rates for the roll and pitch correction values. The stability of the sensor and satellite system as well as the knowledge of the ephemeris and attitude are factors in the length of time for which the assumption that the errors in the imagery are biases holds. The accuracy of the control points may require the use of a filter to reduce the error inherent in the control information. Thus, the number of control points as well as their sources may need to be greatly increased depending on the accuracy of the control. The percentage of cloud cover over a region and the number of control points are directly related, due to the probability that a given control point may be covered by a cloud.

IV. Research topics

Much of the discussion to this point has been based on the experience of the staff at the EROSData Center with the Landsat 2, 3 MSS GCPLIB, the Landsat 4, 5 MSS and TM GCPLIBs and various reference images of AVHRR imagery. The Landsat libraries have been of limited use and are not currently used in a production process at EDC. These are path-oriented (not map projected) and the libraries are static. The use of reference imagery with AVHRR registrations has been very successful and is used in an automated production process at EDC. The reference imagery for AVHRR is merely a map projected reference image with acceptable registration. The matching process extracts chips from it rather than from a GCPLIB.

For EOS sensors and the Landsat 7 project, the GCPLIB concept is being considered on a global basis. The collection, marking, and maintenance of a global GCPLIB for multiple sensors could be an enormous task. The following ideas may simplify the task a bit, or at least tend to eliminate redundant efforts.

1. Consider multisensor/multiresolution registrations. High resolution data lends itself to control selection better than low resolution imagery does, as more man made features are visible. One could select points from a map or from ground/GPS measurements and mark, for example, Landsat TM imagery or aircraft digital orthophotos and rectify these imagery to a map projection. These imagery can then be degraded in resolution (in a sensor-friendly way) and scale changed (low pass filtering followed by down-sampling [Burt and Adelson, 1983]) to a point where they match the resolution of the imagery being registered. In these cases, errors in registration due to control point marking become very small. The largest remaining error is usually due to the matching algorithm, which on a point-by-point basis can be in the 1/4 pixel range (Cracknell and Paithoonwattanakij, 1989; Rignot and others, 1991). The main disadvantage to this type of processing is that 32 by 32 or 64 by 64 image chips are too small and more source imagery is required for the resolution/scale changes of the process. However, this method could allow multiple sensors to share the cost associated with the building and maintenance of a GCPLIB.

2. Other sources of control information such as scanned maps and vector data could be used to correct imagery. The AVHRR processing system at the EROS Data Center uses vector data in an automated fashion to register AVHRR imagery (Eidenshink and others, 1993). Both the scanned maps and the vector-to-raster matching process are current research topics at EDC.

3. For EOS, consider the distribution of updated satellite information (ephemeris, etc.) based on the registration of the higher resolution sensors. This updated location info could benefit the lower resolutions sensors, possibly eliminating the need for ground control in the lower resolution sensors.

V. Implementations options

Before the design of a GCPLIB can be completed and the feasibility of such a library estimated, the various instrument and science groups need to define a registration accuracy and an estimate of how much ground control

will be required to obtain this accuracy. Consideration should be given to pass processing, multisensor/resolution processing (the sharing of resources described above), and cloud cover probabilities. Once the number of control points needed per scene or pass is estimated, this estimate should be extended to estimate the number of GCPs required for global image processing. The next task is to determine how this ground truth will be collected and from what sources.

A. Fully populated and validated GCP libraries

The ideal GCP library for a given satellite/sensor system would be fully populated with precision corrected image chips of sufficient number and distribution to support an automated correction processing operation and ensure as consistent a level of accuracy as possible across all scenes. Such libraries require significant resources to develop and maintain. Typically, each point must be hand picked and validated. The actual number and distribution of these points will vary from system to system and be dependent on factors such as the type of chips and correlation being employed, the resolution of the system, and whether the processing is orbital-segment- or scene-based. For global coverage systems, the population and validation of control points for some remote or poorly mapped geographic regions can be particularly challenging. Although other data sources can serve as the source for control point chips, the ideal source is a sensor system's own data which, of course, delays the availability of a fully populated library for some time after launch. Also, such libraries require continual update to maintain accuracies.

B. Partially populated and validated GCP libraries

Such libraries would also be populated with precision corrected image chips of sufficient number and distribution to support an automated correction processing operation and ensure as consistent a level of accuracy as possible, but only for portions of the full geographic extent of the satellite/sensor system. The population of such libraries could be accomplished by geographic regions, such as countries or continents, or by scientific study areas. The guidelines and procedures for developing and maintaining partial coverage libraries would be the same as for the full coverage libraries allowing them to evolve to become a fully populated library.

C. User provided and validated GCP sets

In such cases, users are given the option of supplying their own GCP set(s) to the data producer for application during user product generation. The

data producer will typically place limits on the format any type of control points accepted. The data producer might maintain an informal library of contributed GCP sets supplied by users but will not give any guarantees regarding accuracy. The accuracy of the contributed control points is the responsibility of the user, but once validated by the data producer, these user contributed GCP sets could become part of a formal partially populated and validated GCP library.

VI. References

Burt, P., and Adelson, E., 1983, The Laplacian Pyramid as a compact image, IEEE Transactions on Communications, COM-31(4), 532-540.

Cracknell, A.P., and Paithoonwattanakij, K., 1989, Pixel and subpixel accuracy in geometrical correction of AVHRR imagery, International Journal of Remote Sensing, 19(4/5), 661-667.

Eidenshink, J.C., Steinwand, D.R., Wivell, C.E., Hollaren, D.M., and Meyer, D.J., 1993, Processing techniques for global land 1-km AVHRR data, Proceedings of Pecora 12 Symposium on Land Information from Space-based Systems, August, 1993.

Hogan, Markarian, Shipman, and Spieler, 1980, GCP location enhancement study, IBM Corporation, NASA Contract NAS5-25509, Goddard Space Flight Center.

Kiss, P., Arnold, P., and Golstine, J., 1981, Image registration system in the Landsat-D production environment, Proceedings of the 1981 Machine Processing of Remotely Sensed Data Symposium.

Pearson, J., Hines, D., Golosman, S., and Kuglin, C., 1977, Video-rate image correlation process, SPIE, 119, 197-205.

Rignot, E., Kowk, R., Curlander, J., and Pang, S., 1991, Automated multisensor registration: Requirements and techniques, Photogrammetric Engineering and Remote Sensing, 57(8), 1029-1038.

Thormodsgard, J.M., and DeVries, D.J., 1983, Geocoding accuracy of Landsat 4 multispectral scanner and thematic mapper data, Proceedings Landsat 4 Science Characterization Early Results Symposium, pp. 132-142.

Welch, R., and Usery, E.L., 1994, Cartographic accuracy of Landsat 4 MSS and TM image data, IEEE Transactions on Geoscience and Remote Sensing, GE-22(3), 281-288.

Wood, L., and Sellman, A.N., 1987, State of the art survey of automated registration and control point chip library systems, Final report number 323901-1-F, ERIM, Ann Arbor, Michigan, August.

APPENDIX 6-5

UNITED STATES NATIONAL MAP ACCURACY STANDARDS
(EXTRACTED FROM BUREAU OF THE BUDGET, 1947)

With a view to the utmost economy and expedition in producing maps which fulfill not only the broad needs for standard or principal maps, but also the reasonable particular needs of individual agencies, standards of accuracy for published maps are defined as follows:

1. Horizontal accuracy. For maps on publication scales larger than 1:20,000, not more than 10% of the points tested shall be in error by more than 1/30 inch, measured on the publication scale; for maps on publication scales of 1:20,000 or smaller, 1/50 inch. These limits of accuracy shall apply in all cases to positions of well-defined points only. Well-defined points are those that are easily visible or recoverable on the ground, such as the following: monuments or markers, such as bench marks, property boundary monuments; intersections of roads, railroads, etc.; corners of large buildings or structures (or center points of small buildings); etc. In general, what is well-defined will also be determined by what is plottable on the scale of the map within 1/100 inch. Thus, while the intersection of two road or property lines meeting at right angles, would come within a sensible interpretation, identification of the intersection of such lines meeting at an acute angle would obviously not be practicable within 1/100 inch. Similarly, features not identifiable upon the ground within close limits are not to be considered as test points within the limits quoted, even though their positions may be scaled closely upon the map. In this class would come timber lines, soil boundaries, etc.

2. Vertical accuracy, as applied to contour maps on all publication scales, shall be such that not more than 10% of the elevations tested shall be in error more than one-half the contour interval. In checking elevations taken from the map, the apparent vertical error may be decreased by assuming a horizontal displacement within the permissible horizontal error for a map of that scale.

3. The accuracy of any map may be tested by comparing the positions of points whose locations or elevations are shown upon it with corresponding positions as determined by surveys of a higher accuracy. Tests shall be made by the producing agency, which shall also determine which of its maps are to be tested, and the extent of such testing.

4. Published maps meeting these accuracy requirements shall note this fact in their legends, as follows: "This map complies with National Map Accuracy Standards."

5. Published maps whose errors exceed those aforestated shall omit from their legends all mention of standard accuracy.

6. When a published map is a considerable enlargement of map drawing (manuscript) or of a published map, that fact shall be stated in the legend. For example, "This map is an enlargement of a 1:20,000-scale map drawing", or "This map is an enlargement of a 1:24,000-scale published map".

7. To facilitate ready interchange and use of basic information for map construction among all Federal mapmaking agencies, manuscript maps and published maps, wherever economically feasible and consistent with the use to which the map is to be put, shall conform to latitude and longitude boundaries, being 15 minutes of latitude and longitude, or 7-1/2 minutes, or 3-3/4 minutes in size.

APPENDIX 6-6

DEFINITION OF ROOT MEAN SQUARE ERROR WITH RESPECT TO CARTOGRAPHY

Extracted from American Society for Photogrammetry and Remote Sensing, 1990

The "root mean square" (rms) error is defined to be the square root of the average of the squared discrepancies. In this case, the discrepancies are the differences in coordinate or elevation values as derived from the map and as determined by an independent survey of higher accuracy (check survey). For example, the rms error in the X coordinate direction can be computed as:

$$rms_x = \sqrt{D^2/n}$$

where:

D^2 = $d_1^2 + d_2^2 + ... + d_n^2$

d = discrepancy in the X coordinate direction

= $X_{map} - X_{check}$

n = total number of points checked on the map in the X coordinate direction

APPENDIX 6-7

ASPRS ACCURACY STANDARDS FOR LARGE-SCALE MAPS
Extracted from American Society for Photogrammetry and Remote Sensing, 1990.

1. Horizontal Accuracy:

Horizontal map accuracy is defined as the rms error in terms of the project's planimetric survey coordinates (X,Y) for checked points as determined at full (ground) scale of the map. The rms error is the cumulative result of all errors including those introduced by the processes of ground control surveys, map compilation and final extraction of grund dimensions from the map. The limiting rms errors are the maximum permissible rms errors established by this standard. These limiting rms errors for Class 1 maps are tabulated in Table 1E (feet) and Table 1M (meters) along with typical map scales associated with the limiting errors. These limits of accuracy apply to tests made on well-defined points only.

Table 1E. Planimetric coordinate accuracy requirement (ground X or Y in feet) for well-defined points - Class 1 maps

PLANIMETRIC (X OR Y) ACCURACY (limiting rms error, feet)	TYPICAL MAP SCALE
0.05	1:60
0.1	1:120
0.3	1:360
0.4	1:480
0.5	1:600
1.0	1:1200
2.0	1:2400
4.0	1:4800
5.0	1:6000
8.0	1:9600
10.0	1:12000
16.7	1:20000

Table 1M. Planimetric coordinate accuracy requirement (ground X or Y in meters) for well-defined points - Class 1 maps

PLANIMETRIC (X OR Y) ACCURACY (limiting rms error, meters)	TYPICAL MAP SCALE
0.0125	1:50
0.025	1:100
0.050	1:200
0.125	1:500
0.25	1:1000
0.50	1:2000
1.00	1:4000
1.25	1:5000
2.50	1:10000
5.00	1:20000

2. Vertical Accuracy:

Vertical map accuracy is defined as the rms error in elevation in terms of the project's elevation datum for well-defined points only. For Class 1 maps the limiting rms error in elevation is set by the standard at one-third the indicated contour interval for well-defined points only. Spot heights shall be shown on the map within a limiting rms error of one-sixth of the contour interval.

3. Lower-Accuracy Maps:

Map accuracies can also be defined at lower spatial accuracy standards. Maps compiled within limiting rms errors of twice or three times those allowed for a Class 1 map shall be designated Class 2 or Class 3 maps respectively. A map may be compiled that complies with one class of accuracy in elevation and another in plan. Multiple accuracies on the same map are allowed provided a diagram is included which clearly relates segments of the map with the appropriate map accuracy class.